Energy & Buildings 366 (2026) 117691

Contents lists available at ScienceDirect

Energy & Buildings

journal homepage: www.elsevier.com/locate/enb

Improving energy efficiency while reducing anthropogenic heat from buildings: how retrofits influence the building stock and urban microclimate in Los Angeles

Yujie Xu, Pouya Vahmani, Andrew Jones, Tianzhen Hong *

Lawrence Berkeley National Laboratory, 1 Cyclotron Road, Berkeley 94720, CA, USA

ARTICLE INFO

Keywords:
Anthropogenic heat
Energy retrofit
Microclimate
Building simulation
Urban cooling
EnergyPlus

ABSTRACT

Anthropogenic heat (AH) from buildings contributes to urban overheating, especially during heat waves, yet building retrofit studies usually evaluate energy savings without assessing impacts on AH. This study quantifies how common building retrofit measures affect both building energy use and AH emissions across the City of Los Angeles. Using a bottom-up urban building energy modeling framework coupled with high-resolution local weather from the Weather Research and Forecasting model with Building Effect Parameterization (WRF-BEP), we evaluate eleven retrofit measures and two multi-measure retrofit packages. HVAC and LED lighting retrofits provide the largest city-wide annual site energy savings, while roof coating is most effective for reducing AH. A package optimized for energy savings reduces summer site energy use by about 32% (2.3 TWh), while a package incorporating AH-focused measures reduces the total AH by over 50% (137 PJ) with minimal difference in energy savings. The AH-aware package produces substantially greater urban cooling, reducing mean near-surface air temperature by up to 0.62 ℃ and peak temperature by up to 3.79 ℃. These results show that retrofit strategies selected only for energy savings may overlook major opportunities for urban heat mitigation. The study provides a framework for integrating AH into building retrofit planning and urban heat resilience policy.

1. Introduction

1.1. Background and context

Energy efficiency is paramount in efforts to reduce building energy use and peak electric demand. Notably, buildings account for approximately 37% of primary energy consumption in the U.S. [1]. Enhancing energy performance of existing buildings is critical to improving energy resilience and reducing energy bills.

Anthropogenic heat (AH) from the built environment and human activities significantly raises urban air temperatures, contributing to the urban heat island (UHI) effect [2]. This urban air temperature increase contributes to heat stress, reduced outdoor thermal comfort, higher cooling demand of buildings, greater public health risk, and infrastructure and grid strain. AH originates primarily from buildings, transportation, industrial processes, and human metabolism, with buildings accounting for over half of total urban AH [3,4]; Sun et al., 2018). Building AH is highly sensitive to weather changes. During heat waves, higher outdoor temperatures increase building cooling demand, which in turn rejects more waste heat into the ambient from HVAC systems, further escalating ambient temperatures forming a vicious cycle [5]. Therefore, assessing and reducing building AH, especially during urban heat waves, is crucial.

1.2. Related work

1.2.1. Differentiating anthropogenic heat from energy use

Understanding the impact of building retrofits requires distinguishing between the energy a building consumes and the heat it releases to the environment. AH is the waste heat emitted outdoors from energy-using activities and is a complex sum of multiple heat fluxes driven by distinct factors. While this study focuses on building-related AH, it is important to recognize that AH originates from various sources. Literature generally categorizes AH into four primary contributors (Table 1): buildings, transportation, industrial processes, and human metabolism Sailor et al. [6], Sun et al. [7]. Transportation is a major contributor in urban areas, where vehicle engine heat and exhaust emissions elevate near-surface temperatures, especially in congested traffic conditions [8], Sailor et al. [6]. Although industrial activities contribute to AH, quantifying the proportion of energy converted to sensible or latent heat can

* Corresponding author.

https://doi.org/10.1016/j.enbuild.2026.117691
Received 29 January 2026; Received in revised form 18 April 2026; Accepted 21 May 2026
Available online 26 May 2026

Table 1
Anthropogenic heat flux contribution by sector from the literature.

Sector	Contribution Range	Primary Waste Heat Sources	Sources
Buildings	45% – 82%	HVAC (60% of sector), Lighting, Electrical Appliances, Water Heating.	[3,4,7]
Transportation	15% – 35%	Exhaust gas, engine radiation, tire-road friction, braking systems.	Pigeon et al. [10], Smith et al. [11]
Industry	5% – 20%*[1]	Manufacturing processes, data centers, cooling towers, power plants.	Dong et al. [12], Taha [9]
Human Metabolism	2% – 8%	Biological heat release (sensible and latent) from residents.	[3,13]

[1]The contribution of the industrial sector varies greatly by how the city boundary is drawn. Usually the study areas in literature include only the urban core. But if the outskirts and regions with power plants are included, the industrial contribution percentage would be higher.

be challenging [4]. In many dense urban settings, buildings account for the majority of total AH, sometimes exceeding 70%, due to sustained operational loads and HVAC heat rejection Sailor et al. [6,9]. This recognition of AH's multi-sector composition reinforces the need for building-focused mitigation as part of a larger urban heat management strategy.

A foundational framework by Hong et al. [14] decomposes building AH emissions into three primary components: (1) waste heat rejected from HVAC systems (Q_HVAC), (2) heat released from the building envelope via convection (Q_SURF), and (3) heat and moisture emissions from ventilation and air exfiltration (Q_AIR). Each component exhibits unique temporal profiles that do not align with a building's energy use. For instance, Q_SURF, driven by solar radiation, often peaks hours after the maximum cooling demand, as envelope surfaces release heat absorbed throughout the day.

These distinct profiles have important consequences for the urban climate. Luo et al. [15] found that while Q_HVAC is the largest contributor during heat waves, the delayed release from Q_SURF sustains elevated nighttime temperatures, worsening heat stress when vulnerable populations are most at risk due to sleep time with limited or no air-conditioning. Similarly, Xu et al. [16] developed a high-resolution AH simulation framework for Los Angeles County, demonstrating its significant role in modifying urban temperature. Crucially, AH is not merely a passive by-product, it can actively alter the local microclimate and increase night time temperature by up to 3°C. Vahmani et al. [5] showed that building AH emissions elevate outdoor air temperatures, which in turn increase cooling loads, forcing HVAC systems to reject even more heat. This feedback loop is absent from most standard building energy models, which assume a static urban microclimate.

Recognizing these complexities underscores the need to move beyond energy-only metrics when evaluating retrofits of buildings in the city or neighborhood context. The next subsection examines how retrofit analysis has (and has not) incorporated AH considerations.

1.2.2. Retrofit Analysis: a disconnect from the urban microclimate

Recent retrofit studies have broadened their scope beyond energy savings to include occupant comfort, carbon emissions, and other building performance outcomes [17,18], Ma et al. [19]. However, most still treat outdoor climate as a static boundary condition and therefore do not capture how retrofits alter anthropogenic heat emissions or affect the surrounding urban microclimate.

Emerging research has begun to address this disconnect. Ferrando et al. [20] quantified direct reductions in AH from envelope improvements such as cool roofs and high-efficiency HVAC systems, reframing building performance to consider external thermal pollution rather than energy use alone. López-Guerrero et al. [21] extended this concept to urban housing in Latin America, designing interventions that optimize both thermal performance and AH reduction. While these studies represent methodological progress, many still overlook the unintended microclimatic consequences of retrofitting.

A notable example is Maronga et al. [22], who, using high-resolution Large Eddy Simulation for Berlin, found that while retrofitting reduced winter heating demand, it unexpectedly elevated the mean daytime summer temperatures. This highlights how interventions designed to improve energy efficiency can exacerbate local overheating challenges.

1.3. Research objective & scope

This study aims to bridge the critical gap in the existing literature by systematically evaluating the effects of common retrofit strategies on both building energy use and AH emissions. The research is grounded in three core contributions: quantifying how eleven retrofit measures impact both energy use and AH components in building stock of the city of Los Angeles; defining and comparing two distinct retrofit packages, one optimized for energy savings and the other emphasizing AH reductions; and utilizing the Weather Research and Forecasting model coupled with the Building Effect Parameterization urban canopy scheme (WRF–BEP; Skamarock et al. [23], Martilli [24]) to capture neighborhood-scale microclimate variability—which cannot be adequately represented by the standard weather station data—and evaluate how city-wide retrofit modifies AH emissions and near-surface air temperature during heat waves. Through a coupled simulation framework that captures interactions between buildings and their microclimates, this study highlights the necessity of an integrated strategy for energy retrofitting that considers buildings as active participants in the urban climate.

1.4. Structure of the paper

The rest of the paper is structured as follows. Section 2 describes the methodology, including the characterization of the Los Angeles building stock, development of the prototype EnergyPlus models, selection of retrofit measures, and configuration of the WRF–BEP framework used to represent local summer microclimate conditions. Section 3 presents the results in two stages: Stage 1 evaluates the individual retrofit measures and defines the retrofit packages using typical weather data, and Stage 2 examines city-wide energy, anthropogenic heat, and air-temperature impacts under high-resolution local weather conditions. Section 4 discusses the main findings, with emphasis on trade-offs between energy savings and AH reduction, spatial and building-type variability, and implications for retrofit planning and urban heat mitigation policy. Section 5 concludes with the main contributions, policy relevance, study limitations, and directions for future research.

2. Methodology

This study integrates bottom-up building energy modeling with high-resolution urban microclimate simulations to assess the impact of building retrofit measures on city-wide energy use and anthropogenic heat (AH) emissions in the city of Los Angeles. The approach combines detailed building stock characterization, prototype model retrofit scenario development, and numerical weather modeling to evaluate both annual performance under typical weather conditions and summer-season behavior under spatially variable, high-resolution climate data. In Stage 1, individual energy conservation measures (ECMs) are tested using typical weather data to determine their relative energy savings potential across the building stock using the EnergyPlus simulation engine. In Stage 2, the most effective measures are combined into a retrofit package and assessed under fine-scale WRF climate data for summer conditions, capturing the influence of local microclimates on retrofit effectiveness.

The following subsections describe the study area, building stock data, climate model configuration, selected retrofit measures, and the calculation procedures for building energy use and AH emissions.

2.1. Research design

Fig. 1 illustrates the overall workflow of the data integration and simulation. Building stock data includes key parameters such as floor area, use type, construction vintage, and building height. To represent the diversity of real buildings without modeling each individually due to intensive computing needs, the building stock was simplified by grouping buildings according to major use types and construction vintages. This reduction was based on a categorical cross-tabulation of these classes, rather than an unsupervised clustering procedure, yielding 54 prototype building models. These models were adapted from the U.S. Department of Energy (DOE) commercial prototype building models and residential buildings from the CBES tool [25]. The prototypes cover 18 distinct building types (e.g., Medium Office, Midrise Apartment, Retail) across three construction vintages representative of the Los Angeles building stock: Pre-1980, Post-2004, and Post-2013. Each standard prototype includes detailed, pre-defined assumptions for geometry (e.g., floor area, number of stories, window-to-wall ratio), internal loads, occupancy schedules, and baseline HVAC system types and setpoints appropriate for the building's function and vintage. These assumptions are derived from the corresponding building energy efficiency standards: commercial models follow ASHRAE 90.1 standards, while residential models follow California Title 24 standards. All models were configured for ASHRAE Climate Zone 3B, corresponding to Los Angeles. For full transparency and reproducibility, a summary table detailing the sources and key characteristics of each of the 54 prototype models is provided in Appendix 4.

Each prototype is matched to specific building use type and vintage combinations, ensuring coverage of the major categories in Los Angeles' building stock. Hourly energy use and AH emissions for each prototype are simulated using EnergyPlus, a widely used building energy modeling engine. Eleven retrofit measures were selected based on their potential building thermal and energy performance improvements—covering envelope improvements, appliance replacements, HVAC and lighting upgrades—are applied individually to each prototype (see Section 2.4), with workflows implemented via Python scripts editing EnergyPlus input files directly and Ruby script with OpenStudio workflow. Additional workflow details for the HVAC retrofit implementation are provided in Appendix A1 Weather data from Los Angeles International Airport is used for ECM-by-ECM comparisons of retrofit effectiveness in Stage 1.

Retrofit effects are scaled to the city level by weighting based on the building stock composition, allowing actions to be ranked by the annual site energy savings. The five highest-impact actions are combined into a retrofit package, which is then simulated under high-resolution local WRF climate data in Stage 2 to assess summer-season performance. All simulations are executed on the U.S. Department of Energy's NERSC Perlmutter supercomputer.

2.2. Study area

The City of Los Angeles was selected as the case study because it provides a strong setting for evaluating building retrofit impacts on both energy use and anthropogenic heat (AH). The city combines a large and diverse building stock with pronounced spatial variability in summer climate driven by coastal influence, complex terrain, and inland warming. Los Angeles also experiences severe urban overheating during heat waves, making it particularly relevant for studying how retrofit strategies influence both building performance and the urban microclimate. The study covers the City of Los Angeles as of 2018. That summer included a notable heat wave from July 6–8, with extreme temperatures (up to 47°C in some neighborhoods, Fig. 2) that provided an important context for evaluating summer-season retrofit performance.

Building stock characteristics were derived from LA County's Assessor Parcel Data [26] and LARIAC6 building footprints Los Angeles Region Imagery Acquisition Consortium Pictometry International Corp. [27] with processing and integration described in [28]. Buildings in the city of Los Angeles are predominantly residential: single-family and

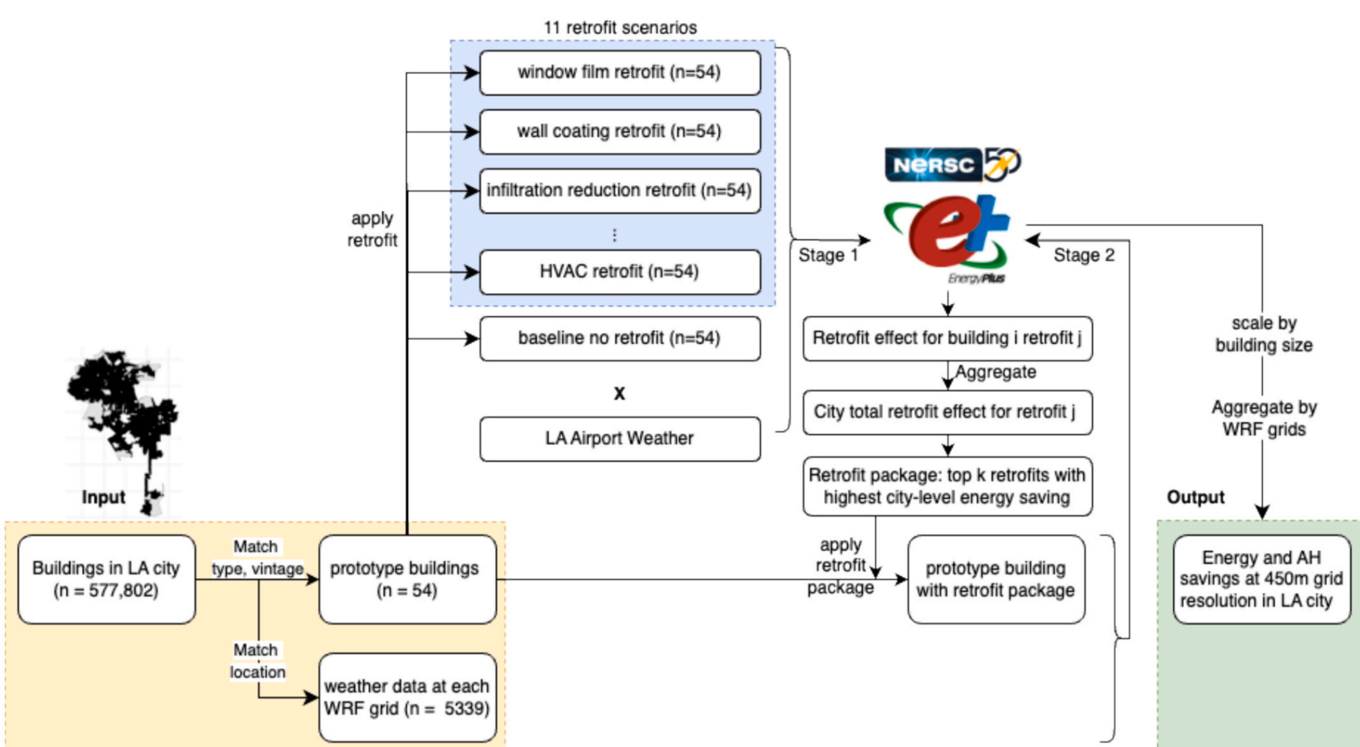

Fig. 1. Illustration of the data integration and simulation workflow.

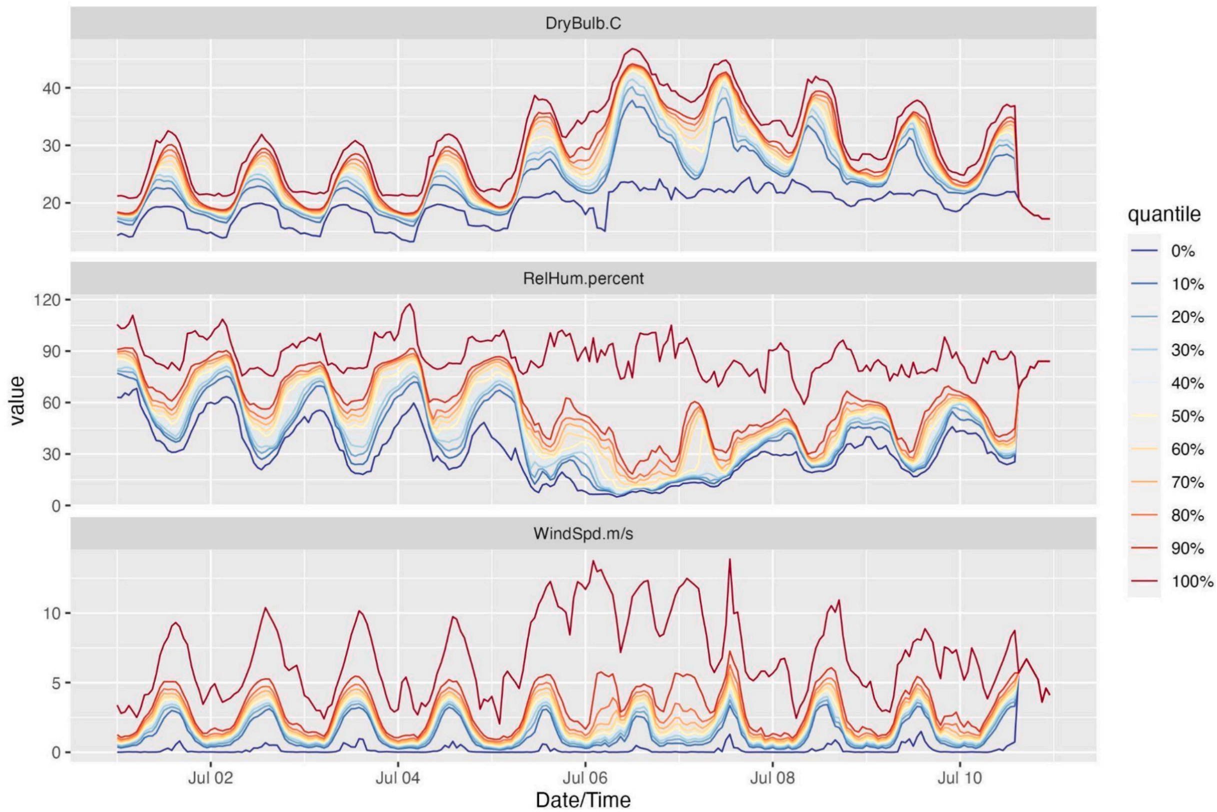

Fig. 2. Distribution of local weather patterns during the 2018 heat wave in Los Angeles city. Top: hourly outdoor air temperature (degree C); Middle: hourly outdoor air relative humidity (%); Bottom: hourly wind speed (m/s).

multi-family buildings account for 73.2% of the total building floor area, followed by commercial buildings (14.7%), industrial (9.5%), and institutional facilities (2.5%) (Fig. 3). The age (year of built) distribution is skewed toward pre-1980 construction, particularly in residential and commercial sectors, where older envelopes and HVAC systems contribute to higher energy use and AH emissions.

2.3. WRF forcing

We simulated the urban climate of the Los Angeles metropolitan

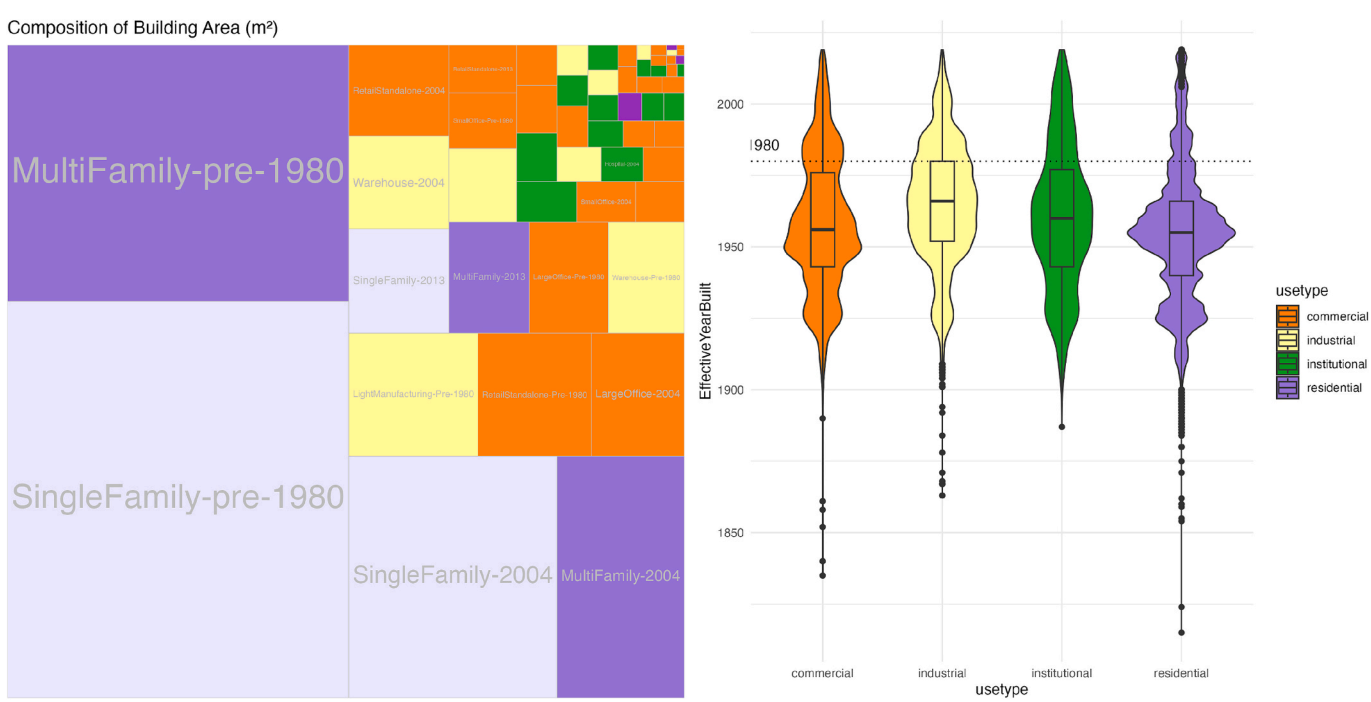

Fig. 3. Building floor area composition (left) and the built year distribution (right) of the building stock in the city of Los Angeles.

region with the Advanced Research Weather Research and Forecasting model (WRF v4.5.2; [23]) coupled to the multi-layer Building Effect Parameterization (BEP) [29]. The configuration used four nested domains with horizontal grid spacings of 12 km (d01), 4 km (d02), 1.3 km (d03), and 0.44 km (d04, 444 m). All nests shared 33 vertical levels and a model top at 50 hPa (p_top_requested = 5,000 Pa). The outermost domain spans the contiguous United States, the intermediate nests focus on Southern California, and the innermost nest resolves the Los Angeles metropolitan area at sub-kilometer scale with a total of 5339 compute grid cells.

The physics suite included RRTMG for both shortwave and longwave radiation [30], the Bougeault–Lacarrère planetary boundary layer scheme (bl_pbl_physics = 8; Bougeault & Lacarrère, 1989), Thompson microphysics [31], the Monin–Obukhov surface-layer formulation [32], and the Noah land surface model [33,34]. Urban processes were represented with the BEP canopy scheme (sf_urban_physics = 2). Local Climate Zones were enabled to allow built form and surface characteristics to vary among neighborhoods [35]. Initial and lateral boundary conditions for all simulations were taken from ERA5 reanalysis [36]. The WRF–BEP configuration was extended to ingest spatially and temporally varying anthropogenic heat (AH) from buildings, derived from the EnergyPlus simulations of the buildings in each compute grid cell.

We evaluated the WRF model performance against in situ observations. Near-surface air temperature (T2) was evaluated using weather stations; summary spatial metrics and diurnal comparisons are provided in Appendix A3 (Fig. A3). The T2 comparison yielded a RMSE of 1.58°C across the station network, indicating good model skill for near-surface temperature.

Summer mean near-surface ambient temperatures in Los Angeles range from 17°C along the coast to 26°C inland, with an average of 23°C (Fig. 4). Inland areas experience much higher extremes, with summer daily peaks reaching up to 47°C during the heat wave period. Notably, a large share of single-family and multi-family residential buildings are located within these hottest inland zones, underscoring the need for targeted passive and active cooling measures and consideration of AH mitigation in heat-vulnerable neighborhoods. Fig. 4 illustrates the spatial pattern of summer average temperatures across Los Angeles, alongside the distribution of building types.

2.4. Retrofit measures and scenarios

Eleven retrofit measures were selected to represent a broad range of commonly used building improvement strategies. The selection was guided by several criteria: relevance to the Los Angeles building stock and climate; inclusion of a spectrum of costs and implementation efforts; and the ability to compare strategies optimized for energy savings versus those that directly reduce anthropogenic heat. The chosen measures therefore cover both passive and active strategies, including low-cost options such as infiltration reduction, relaxed thermostat setpoints, and efficient appliances, as well as more substantial envelope and HVAC interventions like insulation, cool coatings, and high-efficiency heat pumps (Table 2). The HVAC retrofit in this study primarily represents replacement of gas-based heating systems and heating coils with heat pumps, reflecting a practical electrification-oriented retrofit pathway for the existing building stock. Although the study emphasizes summer AH and overheating, cooling-load mitigation was represented mainly through passive and operational retrofit measures such as reflective coatings, window films, ceiling fans, and thermostat adjustments, which directly affect summer cooling demand and heat rejection. Broad replacement of cooling equipment with higher-efficiency air-conditioning systems was not explicitly modeled here and remains an important area for future study.

2.5. Building energy and anthropogenic heat calculation

For each prototype building, annual site energy use and AH emissions are simulated for both the baseline and retrofit cases using EnergyPlus. Each run employs a building model (idf) describing geometry, envelope properties, occupancy schedules, appliances, and HVAC systems, together with a weather file (epw) derived from WRF output (converted from NetCDF via R and Python scripts). Total site energy use is the sum of electricity and natural gas use. EnergyPlus does not report the total building anthropogenic heat (AH) as a single output variable. In this study, the total AH is derived by summing five EnergyPlus output variables that capture heat released from the building envelope, HVAC

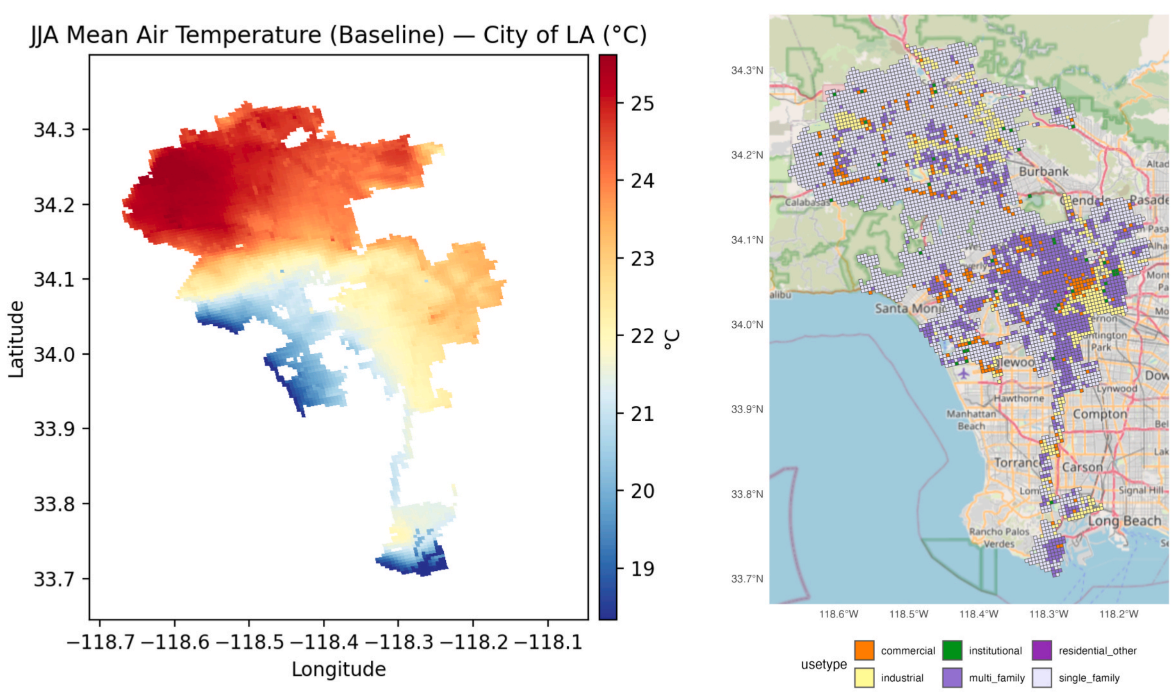

Fig. 4. Map of local ambient air temperature (left), main building type in each grid cell (right).

Table 2
Building Energy Conversation Measures (ECMs) considered for retrofit modeling and analysis.

Category	Retrofit Action	Description	Source
Envelope	window film	Apply a DIY window film to existing windows; change exterior window performance to U-value 4.94 W/m^{2}K, SHGC 0.45, VT 0.66.	(Hong et al. [25])
	wall insulation	Change the insulation layer of exterior walls to R-12 (thickness 0.047 m, thermal conductivity 0.023 W/m·K). If the exterior wall is not insulated, add a R-12 insulation layer to the inside face of the wall.	
	wall coating	Apply cool coating to exterior walls. change exterior layer properties to: solar absorptance 0.4, thermal absorptance/emissivity 0.9.	
	roof insulation	Change the insulation layer of the roof to R-25 (thickness of 0.101 m, thermal conductivity 0.023 W/m·K). If the roof is not insulated, add a R-25 insulation layer to the inside face of the roof.	
	roof coating	Apply cool roof coating. change exterior layer properties to: solar absorptance 0.4 (reflectance 0.6) for residential, 0.15 (reflectance 0.85) for commercial; thermal absorptance/emissivity 0.9.	Vahmani and Jones [37]
	lower infiltration rate	Apply air sealing to reduce infiltration by 30%.	(Hong et al. [25])
Building operation	relaxed thermostat setpoint	Increase summer indoor air cooling setpoint to 28°C.	
	Ceiling or portable fan	Use fan for local cooling, equivalent to relaxing summer cooling setpoint to 28°C; fan power 3 W/m2, air velocity 0.8 m/s.	
Internal loads	LED lighting upgrade	Change lights to LED. Most commercial buildings apply the Comstock measure: set_interior_lighting_technology.	Comstock [38]
	EnergyStar Appliances	Upgrade the following to EnergyStar efficiency: refrigerators (Refrigeration:Case or ElectricEquipment), freezers, washer and dryers.	This study
HVAC efficiency	HVAC	Replacing existing gas boilers, gas heating coils, and gas water heaters to high-efficiency heat pumps. See Table A5 for detailed Coefficients of Performance (COPs).	

systems, and air exchange with the outdoor environment [14]:

1. Environment: Site Total Surface Heat Emission to Air
2. SimHVAC: HVAC System Total Heat Rejection Energy
3. SimHVAC: Air System Relief Air Total Heat Loss Energy
4. Environment: Site Total Zone Exfiltration Heat Loss
5. Environment: Site Total Zone Exhaust Air Heat Loss

These five variables represent the main pathways by which buildings release heat to the outdoor environment. Environment: Site Total Surface Heat Emission to Air captures convective heat transfer from exterior building surfaces to the ambient air. SimHVAC: HVAC System Total Heat Rejection Energy represents heat rejection via cooling towers and/or air-cooled condensers. SimHVAC: Air System Relief Air Total Heat Loss Energy accounts for heat carried away by relief air discharged from mechanical air systems. Environment: Site Total Zone Exfiltration Heat Loss represents heat lost through uncontrolled air leakage from indoor spaces to outdoors. Environment: Site Total Zone Exhaust Air Heat Loss captures heat removed through mechanical exhaust from indoor zones to the outdoor environment.

2.6. Summary

The methodology follows a sequential framework to quantify retrofit impacts on both building energy use and anthropogenic heat emissions across Los Angeles. Detailed parcel and footprint data define the city's building stock by type, vintage, and floor area. Retrofit scenarios of representative prototype building models are developed in EnergyPlus and OpenStudio to simulate hourly energy use and AH emissions for the baseline and retrofit conditions. In Stage 1, each ECM is evaluated individually using typical weather data from Los Angeles International Airport, and the results are scaled to the city level by weighting of the building stock composition. The most effective ECMs are selected to form a retrofit package. In Stage 2, the package is implemented in prototype models and simulated using summer-season, high-resolution local climate data generated by WRF–BEP, allowing performance to be assessed under realistic spatial temperature patterns and meteorological variability. Retrofit effects are aggregated to produce city-wide metrics for both site energy savings and AH reduction, enabling targeted recommendations for energy savings, urban heat mitigation, and public health resilience.

3. Results

This section presents results from both Stage 1 and Stage 2 of the modeling and analysis, quantifying the performance of individual ECMs and selected retrofit packages in terms of city-wide building energy use reductions and changes in building AH emissions. Stage 1 results, based on simulations using typical weather data for Los Angeles, provide an annual baseline comparison across all ECMs and highlight relative performance patterns. Stage 2 results apply high-resolution local WRF climate data to simulate summer-only impacts of selected retrofit packages, capturing the influence of neighborhood-scale variability in weather conditions. The results are organized to first assess the individual ECM impacts on energy and AH, then explore synergies and trade-offs within retrofit packages, and finally analyze spatial and building-type variations to identify strategies with the greatest potential to support both building stock retrofits and urban heat mitigation goals.

3.1. ECM performance Screening with typical weather conditions (Stage 1)

3.1.1. City-wide energy savings by ECM

To assess the effectiveness of the eleven ECMs in terms of energy savings, we simulated both the baseline and retrofitted models for each ECM, using data from the Los Angeles representative weather station at the airport. The difference between the retrofitted and baseline models reflects the retrofit savings, which are then scaled according to the actual building stock composition in Los Angeles. The percentage of total city scale site energy savings serves as the metric for comparing the effectiveness of the ECMs (Table 3).

The HVAC retrofit stands out, achieving the highest annual site energy savings at 16.11%, followed by LED lighting at 10.41%, relaxed setpoint at 4.07%, and ceiling fans at 3.97%. Wall and roof insulation yielded around 3% energy savings, while cool coatings for roofs and walls, infiltration reduction, and EnergyStar measures resulted in savings below 1%. Notably, window film incurred a slight energy penalty annually due to its adverse impact on winter heating, which outweighed the savings gained in summer cooling. This phenomenon is also observed with roof and wall coatings, where cooling energy decreases simultaneously with an increase in heating energy. Such trade-offs are revisited in the subsequent discussion about the impact of ECMs on anthropogenic heat. The HVAC retrofit primarily conserves energy by reducing space heating and domestic hot water energy use, while LEDs

Table 3
City-wide energy and end-use changes from the 11 ECM retrofits (negative values indicating savings or reductions).

ECM	Annual Site Energy	Summer Site Energy	Annual Site Energy End-use Change				
			Cooling	Heating	Lighting	Equipment	Water System
HVAC	−16.11%	−11.32%	−2.08%	−67.44%	0.00%	0.00%	−75.42%
LED	−10.41%	−12.20%	−13.94%	25.27%	−72.16%	0.00%	0.01%
relaxed setpoint	−4.07%	−8.68%	−36.48%	−6.74%	0.00%	0.00%	−0.01%
ceiling fan	−3.97%	−8.50%	−35.72%	−6.63%	0.00%	0.00%	−0.01%
wall insulation	−3.37%	−0.06%	0.03%	−44.44%	0.00%	0.00%	0.00%
roof insulation	−2.23%	−3.00%	−16.43%	−11.13%	0.00%	0.00%	0.04%
roof coating	−0.76%	−3.24%	−19.31%	13.35%	0.00%	0.00%	0.01%
lower infiltration	−0.70%	0.74%	6.05%	−14.99%	0.00%	0.00%	0.00%
wall coating	−0.41%	−2.92%	−19.38%	16.81%	0.00%	0.00%	0.01%
EnergyStar	−0.18%	−0.20%	−0.15%	0.17%	0.00%	−0.07%	0.00%
window film	0.51%	−3.25%	−20.49%	28.67%	−0.14%	0.00%	0.00%

lower annual energy consumption through enhanced lighting efficiency, indirectly reducing emitted heat from improved lighting. Relaxed setpoint, ceiling fans, coatings, and window films primarily aid in reducing cooling loads thus cooling energy. Wall insulation primarily contributes to cooling savings through its role in minimizing solar heat gains, although its impact on heating is limited by conduction and air leakage. In contrast, roof insulation effectively minimizes heat loss in winter and heat gain in summer due to the roof's significant exposure. While infiltration reduction decreases heating consumption by limiting cold outdoor air from entering the building during winter heating season, it can raise cooling demand due to the potential accumulation of internally generated heat during the summer season.

Fig. 5 illustrates the city's total energy usage for a typical week in both summer and winter. The HVAC and LED lighting retrofits significantly reduce energy consumption throughout the day in both seasons, with the relaxed setpoints being particularly effective in summer, notably in reducing afternoon energy consumption. Wall insulation demonstrates higher effectiveness in the winter, particularly in decreasing morning energy use.

3.1.2. City wide building stock AH from the retrofits

As discussed in [16], building anthropogenic heat originates from three main sources: surface convection, HVAC operation (including heat rejection and relief air), and zone air exchange through exfiltration and exhaust.

Table 4 shows the effects of various retrofit strategies on AH, highlighting that roof coating is the most effective method, yielding an overall AH reduction of 52.78%. This strategy significantly decreases Surface AH by 57.30%, and also leads to notable reductions in HVAC AH (18.62%) and Zone AH (26.62%). Other strategies, such as wall coating and relaxed setpoints, show moderate impacts with total AH reductions of 8.55% and 1.52%, respectively.

In contrast, interventions like LED lighting, window film, and reduced infiltration yield minimal AH reductions, often less than 1%. Although some retrofits effectively diminish HVAC AH, others,

Table 4
City-wide energy and AH changes due to retrofits (negative values indicating savings or reductions).

Retrofit	Summer AH percent changes				
	Total AH	Surface AH	HVAC AH	Zone AH	Peak AH
roof coating	−52.78%	−57.30%	−18.62%	−26.62%	−52.54%
wall coating	−8.55%	−8.43%	−17.47%	0.51%	−5.68%
relaxed setpoint	−1.52%	0.38%	−41.01%	18.04%	−0.66%
ceiling fan	−1.49%	0.37%	−40.39%	17.97%	−0.63%
roof insulation	−1.00%	1.88%	−17.12%	−24.47%	−0.11%
LED lighting	−0.89%	−0.10%	−11.32%	−0.01%	−0.45%
window film	−0.84%	0.48%	−19.42%	2.07%	−0.57%
lower infiltration	−0.30%	0.35%	5.01%	−16.52%	−0.19%
wall insulation	−0.06%	−0.13%	0.17%	0.84%	0.31%
HVAC	−0.05%	0.00%	−0.55%	−0.12%	0.00%
EnergyStar	−0.02%	0.00%	−0.29%	0.01%	−0.01%

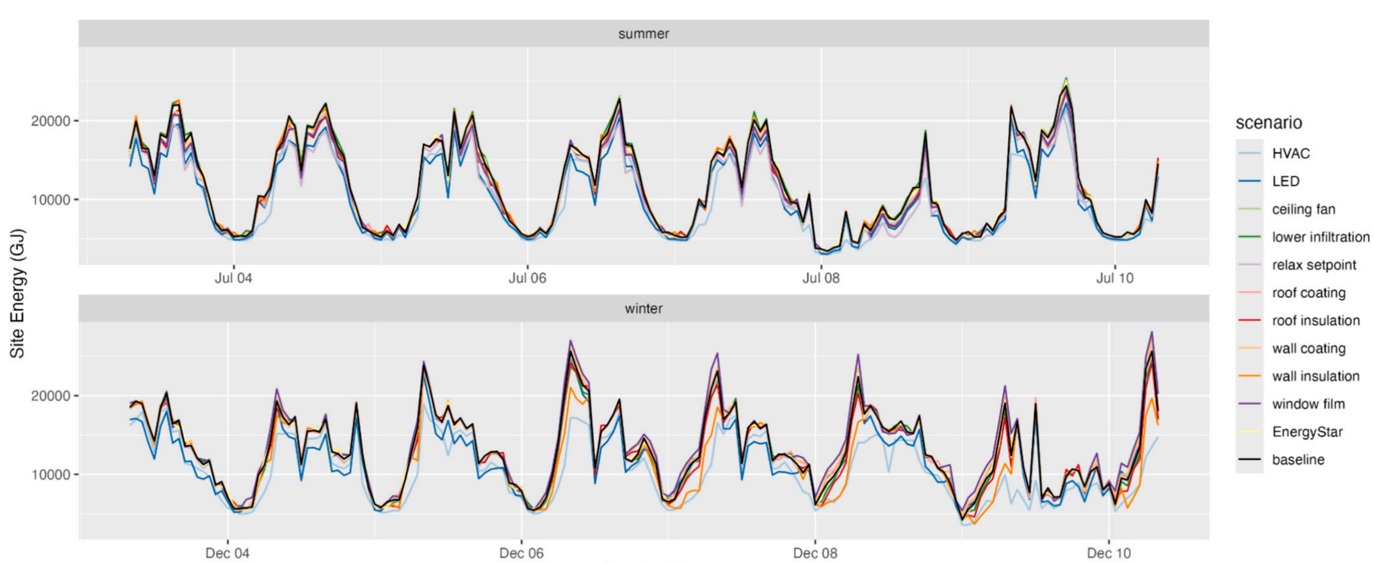

Fig. 5. City-wide energy use comparison in a representative week in summer (July 3 to 10) and winter (December 3 to 10).

including wall insulation and EnergyStar, exhibit negligible effects, suggesting that the efficacy of these strategies can vary considerably. This analysis emphasizes the necessity of selecting appropriate interventions to effectively mitigate AH while balancing occupant comfort and energy efficiency.

Fig. 6 compares the profiles of three AH components during a summer week, revealing that roof coating is particularly effective in minimizing surface AH compared to other retrofits. The relaxed setpoint shows the greatest efficacy in reducing mid-day HVAC-induced AH peaks in summer; however, it inadvertently increases AH from zone air exchange due to indoor temperatures being lower than outdoor temperatures, leading to greater heat absorption through indoor-outdoor air exchange. By increasing the setpoint, the indoor-outdoor temperature difference is reduced, which inadvertently raises AH. Conversely, roof and wall coatings are effective in decreasing AH from zone air exchange.

3.1.3. *Selection of top ECMs for retrofit packages*

Our objective is to select two packages that rank within the top five for energy savings. Notably, both the relaxed setpoint and ceiling fans exhibit similar energy savings; however, ceiling fans are favored due to their enhanced comfort over relaxed setpoints. Table 5 summarizes the performance of these individual ECMs, illustrating their percentage impact on the annual site energy use and summer total AH alongside the final composition of the two retrofit packages. If the selection focuses solely on annual energy savings, the chosen retrofits are HVAC, LED lighting, ceiling fan, wall insulation, and roof insulation. In contrast, if the selection prioritizes AH reduction, roof coating, wall coating, ceiling fan, roof insulation, and LED are selected, with LED lighting, ceiling fan, and roof insulation appearing in both selection sets.

Comparing the seasonal energy use and AH effects of individual retrofits (Fig. 7), coatings and window films are effective in saving energy during spring and summer but increase energy consumption in winter. Meanwhile, envelope coating retrofits have a more pronounced effect on AH reduction, particularly roof coatings. A lower infiltration rate slightly hinders energy consumption, potentially related to the benefits of free cooling from infiltration, especially in mild dry climates with cooler summer nights. Reducing infiltration may limit free cooling, compelling mechanical systems to work harder, thus raising energy consumption in summer. Most retrofits yield the highest energy savings in summer, with HVAC (mainly due to no changes to cooling equipment efficiency for residential buildings) and wall insulation as notable exceptions.

3.1.4. *Performance of packages A and B under typical weather conditions*

We selected two packages: Package A (HVAC + LED lighting + ceiling fan + wall insulation + roof insulation) focuses on the top ECMs for reducing annual energy use, while Package B (HVAC + LED lighting + ceiling fan + wall insulation + roof coating) considers trade-offs between energy use and AH reduction. As noted in Section 3.1.3, roof coating is highly effective in reducing AH but less so for energy savings when assessed on an annual basis. To strike a balance, we included roof coating in Package B while excluding roof insulation, the least effective ECM from Package A, thereby forming Package B.

Table 6 presents the energy and AH changes associated with Packages A and B. Annual site energy savings of about 32% are quite similar between both packages, with Package A achieving slightly higher heating savings and Package B excelling in cooling savings. Notably, both the total and peak AH savings are significantly higher in Package B with minimal change in energy savings but with much more effective AH reductions of more than 50%. It is important to note that individual retrofit effects are not strictly additive. Because building systems interact, applying multiple measures simultaneously generally yields total savings slightly lower than the sum of their individual impacts. A detailed comparison between summed individual effects and the simulated package-level effects is provided in Appendix A2.

Fig. 8 illustrates the hourly energy and AH trends for a typical week across the baseline (black) and the two retrofit packages (red and green). As expected, both packages yield substantial energy savings compared to the baseline in summer and winter. The surface-AH component shows a marked difference, with Package B reducing daily AH peaks by nearly half. For the remaining two AH components, both packages exhibit comparable reductions of similar magnitude.

3.2. *Retrofit package definition*

The specific compositions and performance metrics of the two selected retrofit packages are outlined in Table 7, which details the key effect, driving metric, and individual percentage change for each measure. As illustrated in the table, packages A and B share four ECMs targeting both energy savings and AH reductions, with the only distinction being the inclusion of roof insulation in Package A versus roof coating in Package B. This substitution shifts the package's performance focus: insulation enhances energy performance during both winter and summer, while reflective coating specifically targets summer AH reduction.

In the preceding analysis, we established two distinct retrofit packages to illustrate the trade-offs between energy-focused and AH-aware

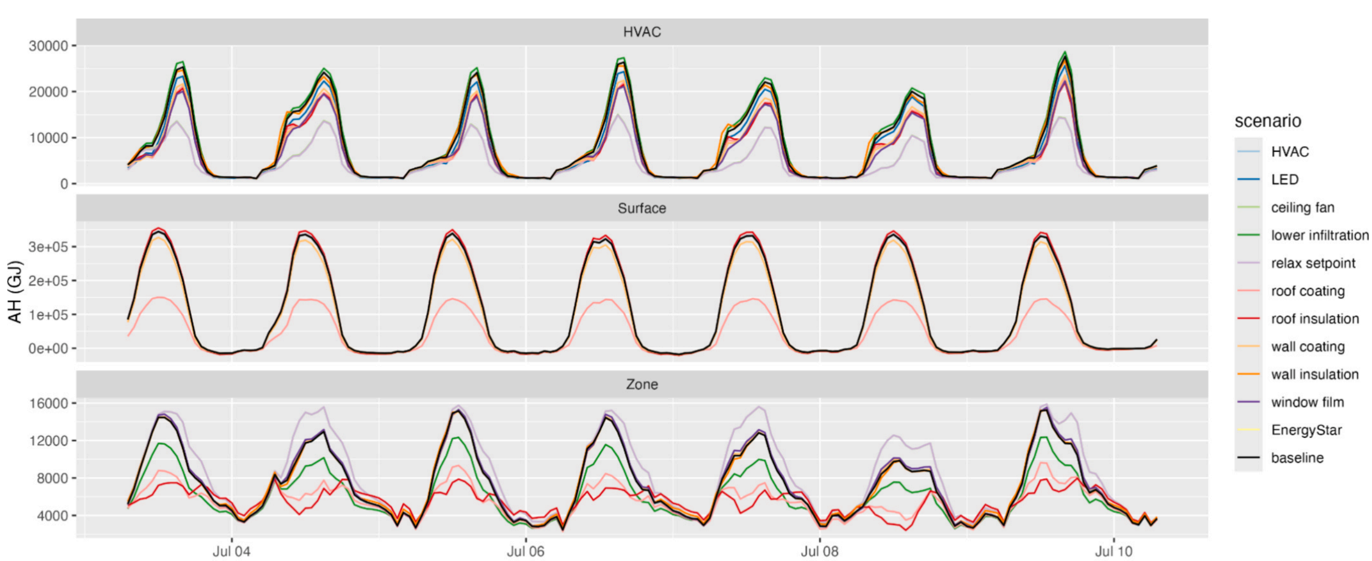

Fig. 6. Comparison of the baseline and retrofit AH components during a summer week.

Table 5
Two retrofit packages with different selection criteria of individual ECMs (negative values indicating savings or reductions).

Retrofit	Annual Site Energy Percent Change	Summer Total AH Percent Change	Prioritize Annual Site Energy Reduction	Prioritize Summer Total AH Reduction
HVAC	−16.11%	−0.05%	x	
LED lighting	−10.41%	−0.89%	x	x
ceiling fan	−3.97%	−1.49%	x	x
wall insulation	−3.37%	−0.06%	x	
roof insulation	−2.23%	−1.00%	x	x
roof coating	−0.76%	−52.78%		x
wall coating	−0.41%	−8.55%		x

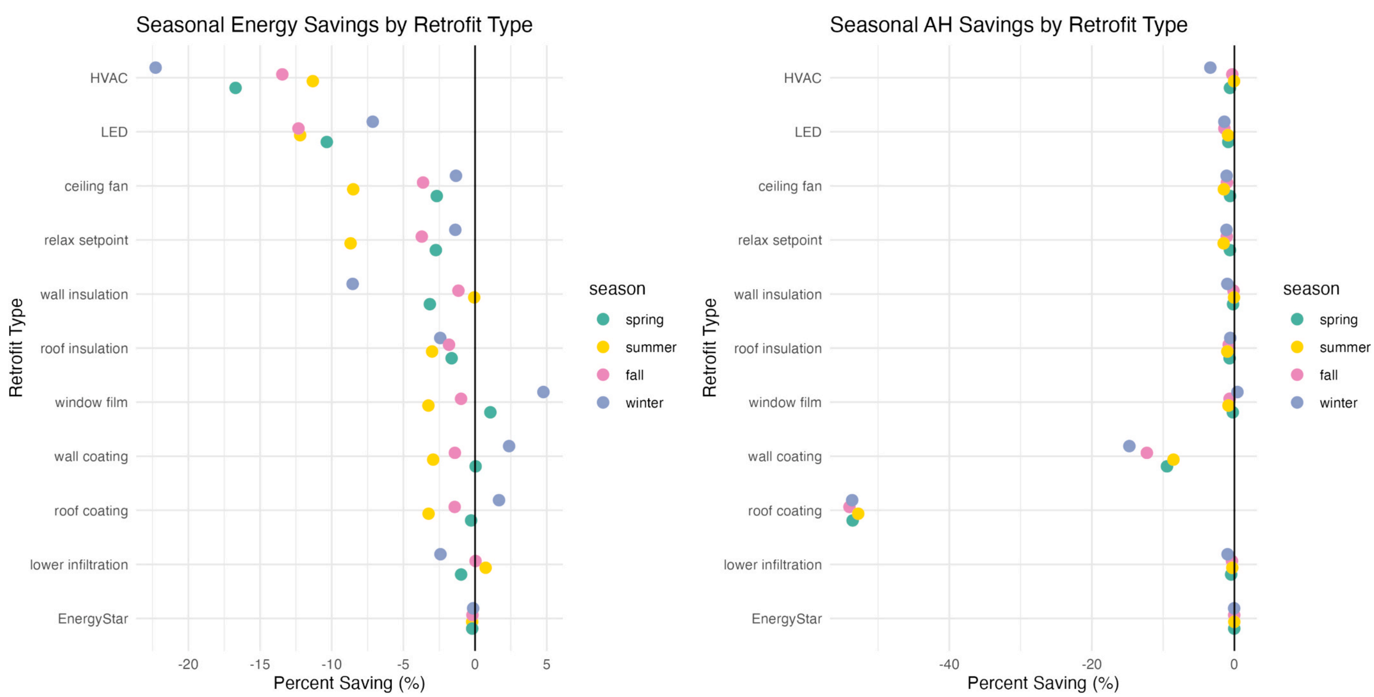

Fig. 7. Comparison of seasonal energy and anthropogenic heat percentage change among the retrofits (negative values indicating savings or reductions).

Table 6
Two retrofit packages with tradeoffs in energy savings and AH changes (negative values indicating savings or reductions).

Metric Type	Metric	Package A Percent Savings	Package B Percent Savings
Energy	Annual Site Energy	−32.41%	−32.04%
	Summer Site Energy	−31.91%	−31.82%
	Cooling end-use	−53.75%	−55.59%
	Heating end-use	−77.74%	−71.02%
	Lighting end-use	−71.37%	−71.37%
	Equipment end-use	0.00%	0.00%
	Water System end-use	−75.07%	−75.08
AH	Summer Total AH	−2.77%	−54.55%
	Summer Peak AH	−0.49%	−52.98%

retrofit strategies. Both packages share a core set of ECMs—HVAC upgrades, LED lighting retrofits, ceiling fans, and wall insulation. However, they diverge in their final envelope measure to reflect different optimization goals. Package A incorporates roof insulation, representing an energy-prioritized pathway. This package was designed to reflect existing municipal policy priorities, providing a critical baseline for how a traditional, energy-first strategy performs. Conversely, Package B substitutes roof insulation with roof coatings, serving as an AH-aware comparison package. Package B is explicitly included in this study to demonstrate how retrofit design—and the resulting impacts on the urban microclimate—shifts when anthropogenic heat mitigation is integrated as a primary objective.

Because fully coupled, high-resolution WRF-BEP city-wide simulations are computationally intensive, it was not feasible to conduct detailed building-type and spatial sensitivity analyses for multiple retrofit packages. Therefore, we selected Package A as the primary subject for the detailed Stage 2 city-wide spatial analysis. This focus was restricted to the summer period, as elevated AH is most critical during this season—exacerbating urban temperatures and driving peak cooling loads—whereas winter AH increases are largely inconsequential for urban overheating. By centering the detailed spatial evaluation on the energy-prioritized baseline (Package A), while retaining Package B to compare macro-level urban cooling effects, this methodological approach allows us to evaluate current policy trajectories while highlighting the distinct value of integrating AH considerations into future urban planning.

3.3. City-wide retrofit scenario results using local weather conditions

3.3.1. City-wide energy savings and AH reductions

Table 8 shows the comparison of using typical weather vs using local weather in the computed percent savings across the grid cells of the city. The energy metric shows very similar percentage savings in site energy (about 32%), lighting, and water systems savings, while the cooling and heating energy savings tend to be overestimated using only typical LA weather. AH metrics also show large differences in the computed

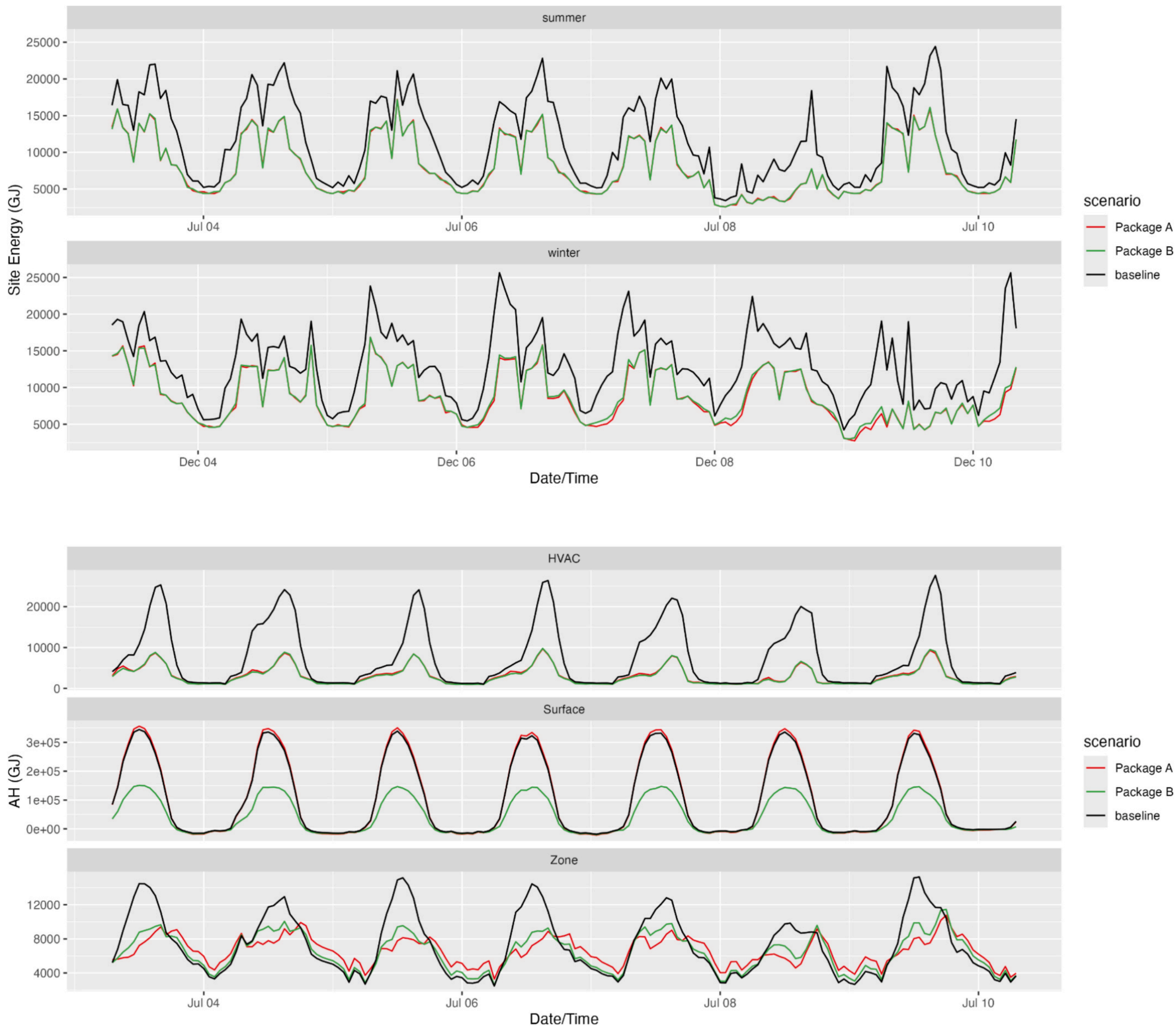

Fig. 8. Retrofit effects on the total site energy by season (top) and summer AH by component (bottom).

Table 7
Definition of the two retrofit packages (negative values indicating savings or reductions).

Retrofit	Key Effect	Driving Metric	Percentage Change (%)	Package A	Package B
HVAC	Reduce heating and cooling energy consumption	Energy	−16.1%	x	x
LED lighting	Reduce lighting electricity consumption	Energy	−10.4%	x	x
Ceiling fan	Improves airflow, reducing cooling energy and HVAC-induced AH	Energy/AH	−4.0%/-1.5%	x	x
Wall insulation	Reduces heating and cooling loads	Energy	−3.4%	x	x
Roof insulation	Reduces heating and cooling loads	Energy	−2.2%	x	
Roof coating	Reflective layer reduces rooftop heat gain, and surface AH	AH	−52.8%		x

savings, where the simulation result of summer time total AH saving is twice using local weather compared with using the typical weather file. The difference in the estimated peak AH reduction is more substantial, changing from 0.5% to close to 4% reduction. These results highlight the importance of incorporating local weather into the modeling and analysis. Fig. 9 compares the daily profiles of site energy use and AH for both the baseline and Package A during a typical summer week. For both metrics, the absolute values peak during the daytime, which is also when Package A delivers the greatest reductions.

3.3.2. Neighborhood patterns — GIS heat maps

Fig. 10 shows the energy and AH percentage changes from the retrofit Package A. Energy savings tend to correlate with the dominant building type. Neighborhoods with high energy savings tend to collocate with single-family dominated neighborhoods. The industrial regions along major highways tend to have lower energy savings due to their dominant process loads not changed by the ECMs. AH reduction seems to correlate with both local weather (Fig. 4 left panel) and building types (Fig. 4 right panel). Regions with higher percent AH reductions can be

Table 8
City-wide energy and AH changes from Retrofit Package A (negative values indicating savings or reductions).

Metric Type	Metric	Package A (%) changes Using Typical Weather, annual	Using Local Weather, summer
Energy Use	Site Energy	−31.78%	−32.21%
	Cooling end-use	−64.43%	−53.71%
	Heating end-use	−61.05%	−48.24%
	Lighting end-use	−71.38%	−72.21%
	Equipment end-use	0.00%	0.00%
	Water System end-use	−75.60%	−75.62%
AH	Summer Total AH	−2.77%	−4.58%
	Summer Peak AH	−0.49%	−3.89%

found in the northern and central part of the city, with higher average temperature and larger concentration of commercial, industrial, and multi-family buildings.

Fig. 11 compares the effects on ambient temperature due to Package A and Package B. We can see the reductions in the mean near-surface air temperature is much greater with Package B which includes roof coatings. In the areas where Package A and Package B have the greatest impact, they respectively reduce the mean air temperature by 0.37°C and 0.62°C, as well as the maximum air temperature by 1.41°C and 3.79°C. When averaged across the entire city, Package A and Package B lead to reductions in mean air temperature of 0.13°C and 0.36°C, respectively, and reductions in maximum air temperature of 0.06°C and 0.75°C. The regions with larger AH reduction (panel b of Fig. 10) also have larger cooling effects (Fig. 11).

3.4. *Influence of building type and local climate on retrofit performance*

Fig. 12 presents the distribution of retrofit impacts on the mean site energy use (left panels) and peak building AH emissions (right panels) across all building types, using Stage 2 results with local WRF weather data. Most building types show clear reductions in site energy up to 69%. The highest percent reductions are achieved in retail stores, single-family homes, small hotels, and mid-rise apartments with around 50% savings. Hospitals and manufacturing facilities are among the lowest energy savers with below 10% savings due to these building types being dominated by process loads that are not changed by the ECMs. Variability in energy savings within each building type is generally modest, though some types exhibit wider ranges due to differences in local weather conditions and microclimate effects captured in the high-resolution simulations.

In contrast, peak AH impacts vary more widely. For most building types, the effect on peak AH clusters near zero, indicating limited shift in average summer heat rejection to the atmosphere. They also show much greater spread for certain building types like super markets. These variations highlight the influence of both local weather and building operational characteristics on retrofit performance, and underscore that peak AH effects can diverge markedly from mean energy trends, even within the same building type.

To formally assess the relationship between retrofit performance and local climate conditions, Fig. 13 presents scatter plots of the mean energy reduction and peak AH reduction against mean summer dry bulb temperature across all building-weather combinations. The Spearman correlation between mean energy reduction and mean summer temperature is negligible ($\rho = 0.01$, $p = 0.068$), confirming that energy savings are largely independent of local climate and are instead driven primarily by building type, consistent with the distinct horizontal banding observed in the figure where each building category maintains a relatively consistent reduction level regardless of the outdoor temperature. In contrast, peak AH reduction shows a statistically significant but weak positive correlation with mean summer temperature ($\rho = 0.03$, $p < 0.001$), suggesting that retrofit impacts on peak AH become slightly more variable and unpredictable in hotter climates, with the spread of outcomes widening noticeably beyond 21°C.

Notably, while energy reductions are consistently negative across all building types, peak AH reductions exhibit both positive and negative values, indicating that some building types such as hospitals and large hotels may experience an increase in peak AH emissions under the retrofit package. This divergence between energy and AH trends underscores that reducing building energy consumption does not necessarily translate to a reduction in peak heat rejection to the atmosphere, and that the two objectives may require different retrofit strategies depending on the building type and local climate context.

4. Discussion

We synthesized the findings from Stage 1 and Stage 2 simulations, highlighting how individual energy conservation measure and aggregated retrofit packages perform in reducing city-wide building energy use and building anthropogenic heat emissions. By comparing results from typical weather data (Stage 1) and high-resolution local summer climate modeling (Stage 2), the analysis reveals how ECM effectiveness varies by season, building type, and microclimate. The sub-sections below review the most impactful strategies for energy and AH reduction, examine synergies and trade-offs in multi-measure retrofit

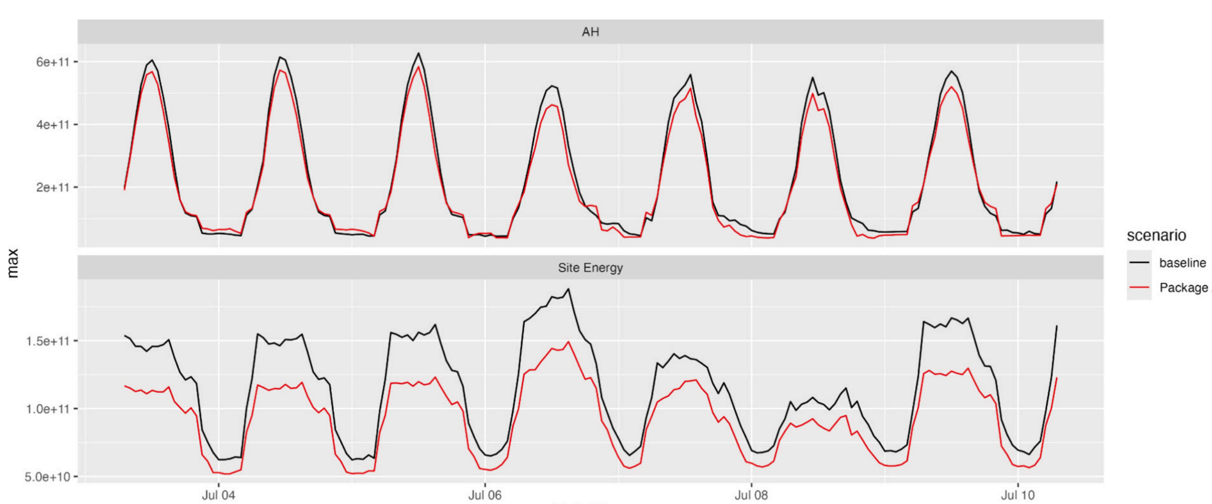

Fig. 9. Peak AH differences between the baseline and retrofit Package A during a typical summer week.

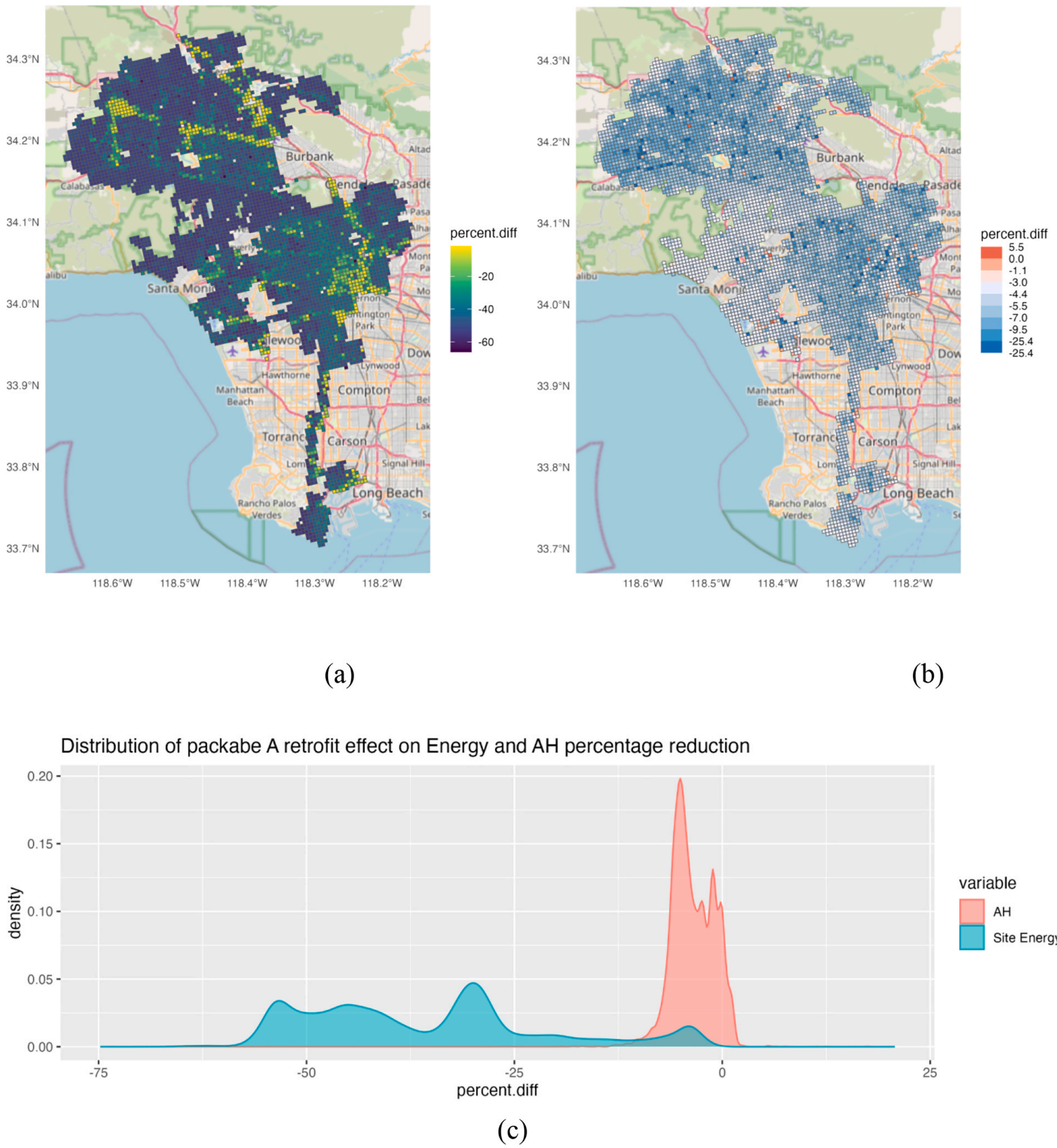

Fig. 10. Comparison of the city-wide percentage changes of the retrofit Package A on energy use and AH: (a) Map of % energy change. (b) Map of % AH change. (c) Distribution of % energy and AH changes.

packages, assess alignment with local policy goals, and conclude with recommendations for short-term and long-term policy design. Limitations of the current study are discussed alongside opportunities for future research, providing a roadmap for integrating AH considerations into urban energy planning.

4.1. Divergent drivers of energy savings and AH reductions

Across all 11 ECMs, HVAC retrofits and LED lighting emerged as the most effective strategies for reducing annual city-wide energy use. In contrast, roof coatings were by far the most effective for mitigating anthropogenic heat, cutting total summer AH emissions by more than half. These contrasting performance profiles underscore a fundamental physical difference in how ECMs interact with the urban environment: energy-optimal ECMs and AH-optimal ECMs operate via different mechanisms and target different components of a building's thermal balance.

As demonstrated by the statistical and spatial analyses in Section 3, the magnitude of energy savings is strongly dictated by a building’s baseline energy end-use profile rather than its local climate. Because the most effective ECMs target specific operational systems (HVAC and lighting), their impact is bounded by what fraction of the building's total energy those systems consume. For instance, retail stores, single-family homes, and mid-rise apartments achieve high percentage savings, whereas hospitals and manufacturing facilities show limited gains (<10%) because their energy consumption is dominated by heavy process loads that remain unaffected by these retrofits. Consequently, energy savings correlate heavily with building typologies.

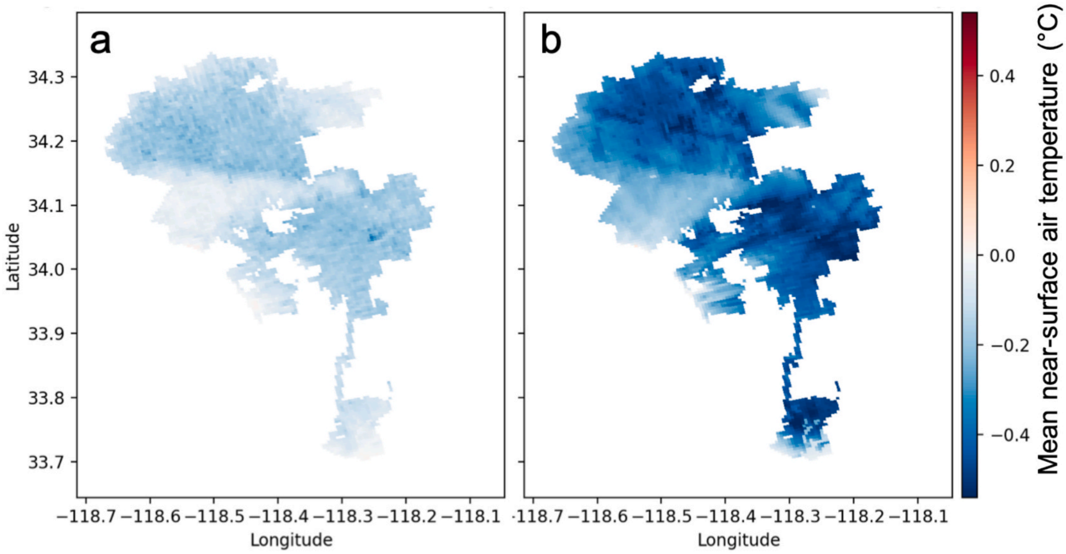

Fig. 11. Changes in the mean near-surface air temperature (retrofit – baseline, °C) over the City of Los Angeles for the two retrofit packages. Panels (a) and (b) show Package A and Package B. Both panels are derived from WRF–BEP simulations for JJA 2018.

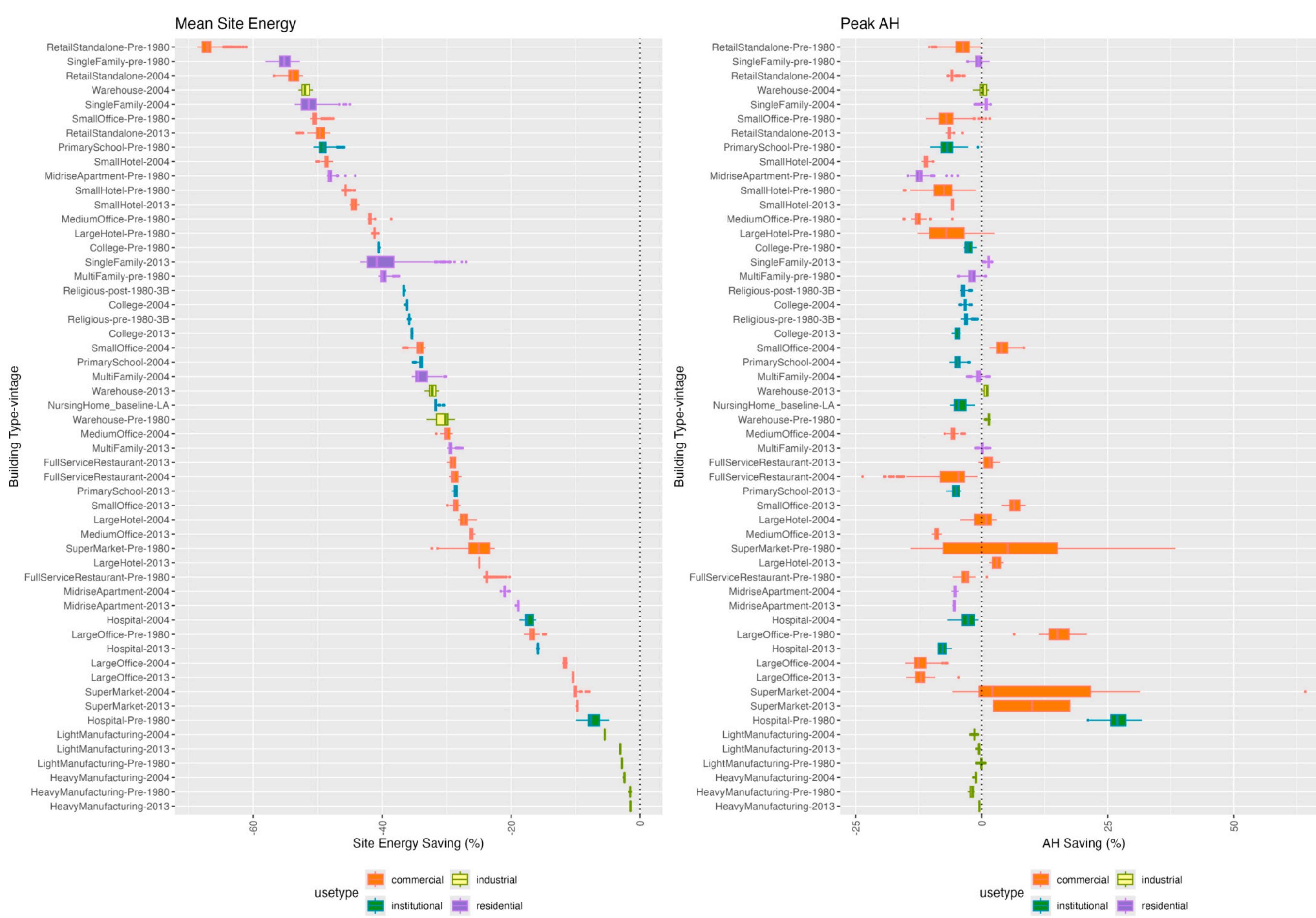

Fig. 12. City-wide distributions of retrofit impact on summer mean site energy and peak anthropogenic heat (right) for all building types under local weather conditions. Negative values indicate percentage reductions relative to the baseline.

Conversely, total AH includes not just building exhaust, but also the convective and radiative heat release from exterior surfaces. Because surface heat release is fundamentally tied to the urban microclimate—dictated by solar incidence, local wind speeds, and ambient temperatures—ECMs targeting the exterior envelope (like roof coatings) yield massive AH reductions. This physical distinction explains why AH reductions exhibit strong spatial heterogeneity and are highly sensitive to local meteorological variations.

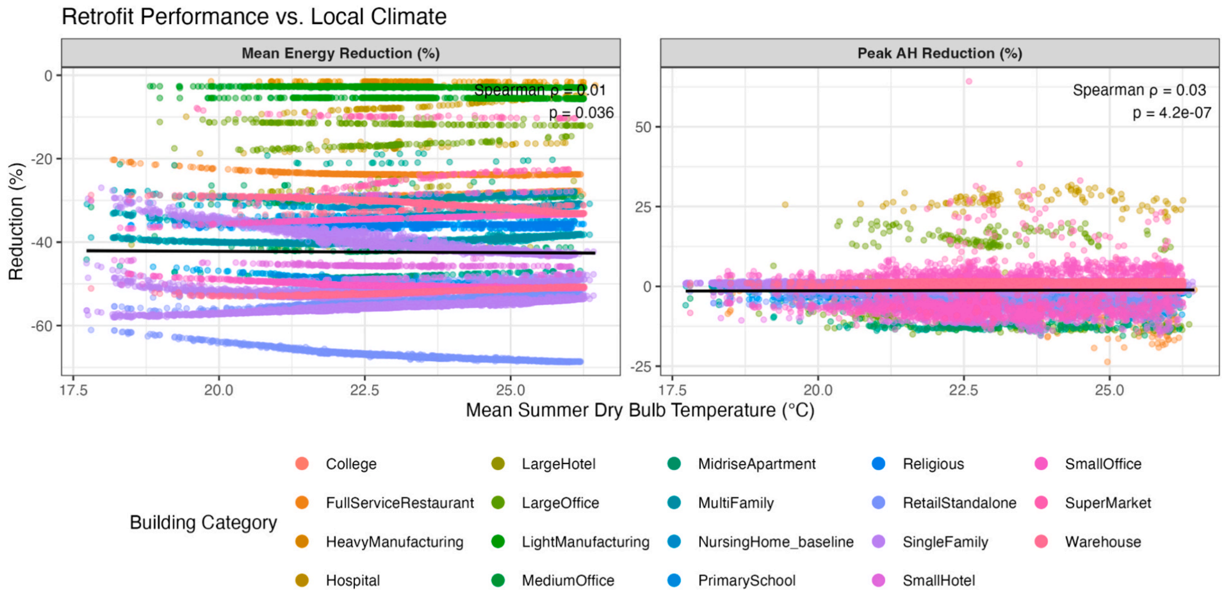

Fig. 13. Retrofit Impact on the Mean Energy Use and Peak AH Reduction versus the Mean Summer Temperature.

This sensitivity is further highlighted when comparing Stage 1 (typical weather) and Stage 2 (local WRF weather) simulations. While percentage energy savings remained consistent across both weather treatments, the summer total AH savings under local weather conditions were nearly double those computed with typical weather data for Package A. Ultimately, these findings indicate that AH is a highly localized phenomenon, and that high-impact urban heat mitigation strategies cannot rely on generalized weather assumptions or energy-centric performance metrics.

4.2. *Synergies and Trade-offs between energy savings and AH reductions*

The formulation of Package A (optimized for energy) and Package B (optimized for AH reduction) highlights a critical tension in urban planning: energy-only optimization can inadvertently sideline substantial urban-cooling benefits. Package A relies heavily on equipment efficiency and insulation (HVAC, LED, ceiling fans, wall/roof insulation). While highly effective for year-round energy efficiency, this combination misses the opportunity to alter the urban radiation balance. Package B, which replaces roof insulation with reflective roof coating, introduces a strong seasonal trade-off, reducing energy use in summer but increasing it in winter, yet it unlocks an order-of-magnitude increase in AH reduction (jumping from under 5% to over 54%).

This dramatic reduction is driven by a dual mechanism: roof coatings reduce not only direct surface AH but also HVAC heat rejection. Physically, this occurs because a more reflective roof reduces solar heat gain into the building, which lowers indoor cooling demand and therefore decreases the amount of waste heat rejected outdoors by the cooling equipment. This mechanism is expected to be strongest in buildings with large roof-area-to-floor-area ratios, such as low-rise commercial and residential buildings, and weaker in taller buildings where roof heat gains account for a smaller fraction of the total cooling load. As a result, the city-wide importance of this effect is heavily influenced by the morphology and building-stock composition of Los Angeles, where many neighborhoods are dominated by roof-exposed low- to mid-rise buildings.

The implications of these physical and morphological dynamics are spatially visualized in the ambient temperature impacts from Section 3. While Package B sacrifices a marginal fraction of annual energy performance compared to Package A, it achieves significantly larger ambient cooling effects across the city (up to 3.79°C reduction in peak temperatures, compared to just 1.41°C for Package A). Furthermore, as mapped in Section 3.3, the regions of the city that experience the greatest ambient cooling align precisely with areas possessing higher concentrations of commercial and industrial buildings.

For policymakers and urban planners, these results suggest that retrofit programs should move beyond single-metric optimizations. A purely energy-driven approach may lead to missed opportunities for mitigating the urban heat island effect, particularly in dense, hotter neighborhoods where thermal stress is highest. By integrating both energy and ambient cooling metrics, city-wide retrofit packages can be tailored to leverage spatial heterogeneity, deploying reflective coatings in heat-vulnerable zones while prioritizing insulation in areas where winter heating penalties outweigh summer cooling benefits.

4.3. *Policy implications*

The city-wide summer simulation results for Package A align closely with the energy efficiency and affordability pathways envisioned in the LA100 Study and the Los Angeles Climate Action and Adaptation Plan (CAP), both of which prioritize reductions in total and peak electricity demand as part of the transition to a 100% renewable grid. Building energy savings from retrofit packages reduce stress on grid operations, directly supporting CAP targets for load flexibility.

However, current CAP metrics focus primarily on carbon and energy, without explicitly accounting for AH emissions. Stage 2 results show that while the mean energy use declines for most building types, peak AH responses vary widely, with some increasing substantially. Elevated AH during peak summer has direct implications for urban heat mitigation: it can raise local ambient temperatures, drive up cooling demand, and increase summer peak loads — potentially counteracting some energy savings. These temperature rises also heighten public health risks during extreme heat events, particularly for vulnerable populations during power outages.

Integrating AH reduction as a performance metric would strengthen the LA100 and CAP pathways by ensuring retrofit strategies advance energy efficiency, mitigate local overheating, and support heat resilience objectives. Policy mechanisms such as targeted incentives, enhanced building performance codes, and rebate programs could accelerate adoption of high-impact retrofit measures. Including AH reductions in incentive criteria would promote urban heat mitigation and associated public health co-benefits.

This analysis equips urban planners with actionable data to select retrofit strategies that simultaneously advance energy reduction goals, lower summer peak demand, mitigate the urban heat island, and improve public health resilience. Policymakers aiming to meet CAP energy targets could prioritize incentive programs for building types and regions with high energy savings potential. To address urban heat, planners could assess local heat vulnerability and prioritize AH reduction measures in high-risk neighborhoods, thereby lowering ambient temperatures and breaking the feedback loop of HVAC reject heat fueling more cooling demand.

The findings support both short-term and long-term planning. In the short term, targeted ECM and retrofit deployment could quickly cut summer energy use, reduce peak loads, and limit local heat exposure, helping prevent grid stress and health impacts during hot weather. In the long term, embedding AH considerations in building codes, incentive frameworks, and energy policies would ensure sustained reductions in cooling demand growth, reinforce the LA100 energy transition, and integrate urban heat resilience into the evolving building stock. By quantifying spatial and seasonal variability, this study enables planners to bridge near-term objectives with long-term energy and climate adaptation goals.

4.4. Limitations and future work

Several limitations influence the scope and interpretation of this study, many of which stem from the intensive computational requirements of physics-based energy and climate simulations. In Stage 1, retrofit impacts were assessed using typical weather data from the LAX airport, which does not capture the variability introduced by local climate conditions. Action-by-action breakdowns under local weather were therefore not available for comparison. Stage 2 simulations, in contrast, applied high-resolution local weather but were restricted to the summer period, leaving full annual and seasonal patterns unexplored. In forming retrofit packages, single-action effects were compared individually, although combined impacts may not be additive. Exploring all possible retrofit combinations at city scale was computationally intractable. Additionally, this study did not assess implementation costs, return on investment (ROI), or other economic metrics, which are essential for practical prioritization.

Future work should address these limitations by developing faster simulation approaches, such as surrogate or reduced-order modeling, to make detailed, city-wide, physics-based analysis more tractable. These methods could enable Stage 2-style local-climate simulations to be extended year-round, permit evaluation of additional ECM combinations, and support staged retrofit pathway analysis. Incorporating economic feasibility metrics, such as cost and ROI, would strengthen decision-making relevance for planners and policymakers. Finally, expanding the scope to integrate building-level retrofit effects with other urban systems such as projected electric vehicle adoption and its associated grid impacts would provide a more comprehensive picture of energy use, anthropogenic heat emissions, and resilience under future urban scenarios.

5. Conclusion

This study quantified the city-wide summer and annual impacts of a range of common adopted energy conservation measures on both building energy use and anthropogenic heat emissions across Los Angeles. The results reveal that ECMs optimized for energy savings are not necessarily the most effective for AH reductions. HVAC and LED lighting retrofits delivered the largest annual site energy savings city-wide, while roof coating achieved the greatest AH reduction, lowering total AH emissions by over 50%. Seasonal trade-offs were evident: measures such as cool coatings and window films reduced cooling loads during summer but increased heating energy use in winter. High-resolution Stage 2 simulations using local WRF climate data showed that AH reduction is more sensitive to microclimate variability than energy savings, with energy impacts tied mainly to building type and AH reductions influenced by both building type and local weather patterns.

Comparison of energy-optimized (Package A) and energy-AH-balanced (Package B) retrofit bundles highlights the potential to significantly enhance urban cooling benefits by adjusting retrofit composition. Package B's substitution of roof coating for roof insulation yielded a modest decrease in energy savings but a substantial rise in AH reduction and city-wide ambient cooling, tripling the peak temperature reduction relative to Package A. These findings underscore the importance of multi-metric optimization: strategies selected solely for energy savings may overlook opportunities to mitigate urban heat and its associated public health risks.

From a planning perspective, integrating AH metrics into the Los Angeles Climate Action Plan and LA100 renewable transition framework would enable policymakers to identify retrofit strategies that simultaneously advance energy targets, limit local overheating, reduce peak cooling demand, and support public health resilience. In the short term, targeting priority ECMs and building types in high-risk neighborhoods can deliver rapid reductions in summer peak loads and local heat exposure. In the long term, embedding AH-aware criteria into building codes, incentives, and energy policies will ensure sustained reductions in cooling demand growth and improve urban climate resilience.

Future work can extend high-resolution analyses beyond the summer period to capture annual patterns, explore compound ECM effects through faster surrogate modeling and simulations, and assess economic feasibility to better inform practical deployment strategies. Although this study focuses on the city of Los Angeles, the methodology, developed using public data, open-source simulation engines, and the available scripts, can be adopted to study building energy use and anthropogenic heat and their interactions and impacts on urban overheating for other cities in the U.S. or internationally.

CRediT authorship contribution statement

Yujie Xu: Writing – original draft, Visualization, Software, Methodology, Investigation, Formal analysis, Data curation. **Pouya Vahmani:** Writing – original draft, Visualization, Software, Methodology, Investigation, Formal analysis, Data curation, Conceptualization. **Andrew Jones:** Writing – review & editing, Supervision, Project administration, Methodology, Funding acquisition. **Tianzhen Hong:** Writing – review & editing, Supervision, Methodology, Conceptualization.

Declaration of competing interest

The authors declare that they have no known competing financial interests or personal relationships that could have appeared to influence the work reported in this paper.

Acknowledgments

This research was supported by the U.S. Department of Energy, Office of Science, as part of research in the MultiSector Dynamics, Earth and Environmental System Modeling Program. This research used resources of the National Energy Research Scientific Computing Center (NERSC), a DOE Office of Science User Facility supported by the Office of Science of the U.S. Department of Energy under Contract No. DE-AC02-05CH11231. The U.S. Government retains, and the publisher, by accepting the article for publication, acknowledges, that the U.S. Government retains a non-exclusive, paid-up, irrevocable, world-wide license to publish or reproduce the published form of this manuscript, or allow others to do so, for U.S. Government purposes.

Appendix

A1. Workflow of HVAC retrofits

In this study, the HVAC retrofit involves replacing existing gas heating systems, including gas heating coils, boilers, and water heaters, with more efficient heat pumps and heat pump water heaters. For most commercial buildings, an OpenStudio model osm) is created with the installation of heat pumps. The generated osm model then applies the "upgrade_hvac_replace_boiler_by_heatpump" measure to substitute gas boilers with heat pump water heaters. After this modification, the osm models are exported into the EnergyPlus input format for subsequent simulations. For building types such as single-family homes, multi-family residences, religious facilities, and nursing homes, those not generated directly from the OpenStudio standard gem, Python scripts are utilized to make direct modifications to the HVAC systems in the EnergyPlus input files. The workflow for the HVAC system upgrade is illustrated in Fig. A1.

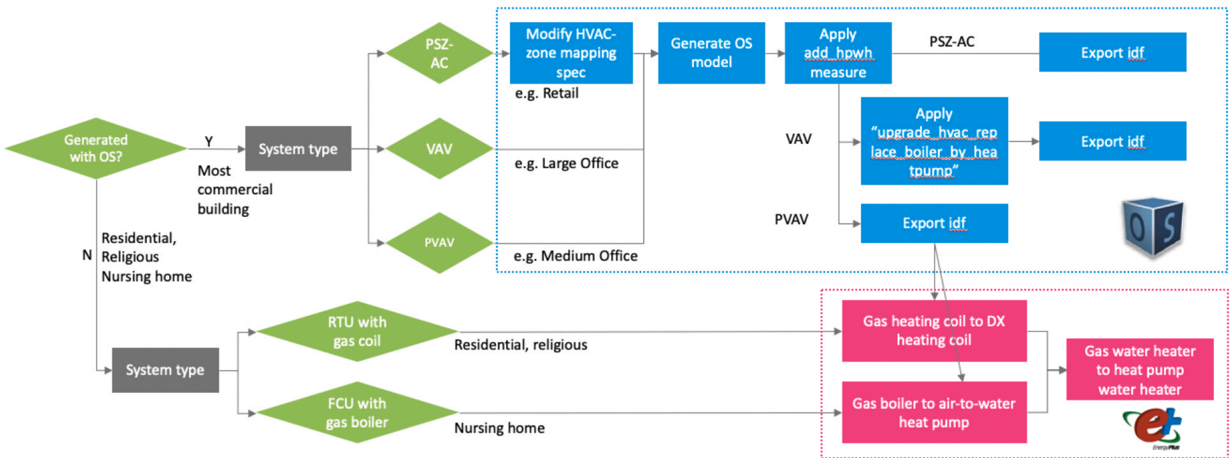

Fig. A1. HVAC retrofit flow diagram

A2. Retrofit effect between individual and package

Fig. A2 compares aggregate savings achieved by summing the savings from individual retrofit actions against the savings realized when these actions are applied collectively as a package. The top row illustrates the cumulative effects of individual actions, while the bottom row shows the outcomes of the retrofit packages. The left column represents annual energy savings, and the right column displays summer anthropogenic heat reductions. Given that anthropogenic heat significantly contributes to outdoor temperature increases, particularly during summer, the analysis of AH is concentrated in this season.

The retrofit effects are not additive for energy savings and anthropogenic heat reductions; in many cases, the retrofit package delivers smaller savings, particularly in buildings like hospitals and large hotels. For instance, added insulation may reduce heating and cooling demands, allowing HVAC systems to operate less intensively to maintain comfort levels. Consequently, in buildings that are already highly energy-efficient, achieving further savings through additional retrofits becomes more challenging. While both packages yield similar energy savings, they can have notably different impacts on anthropogenic heat; Package B, which includes roof coatings, results in significantly higher reductions in summer AH. This underscores the importance of incorporating anthropogenic heat considerations into retrofit decision-making for a more comprehensive understanding of overall.

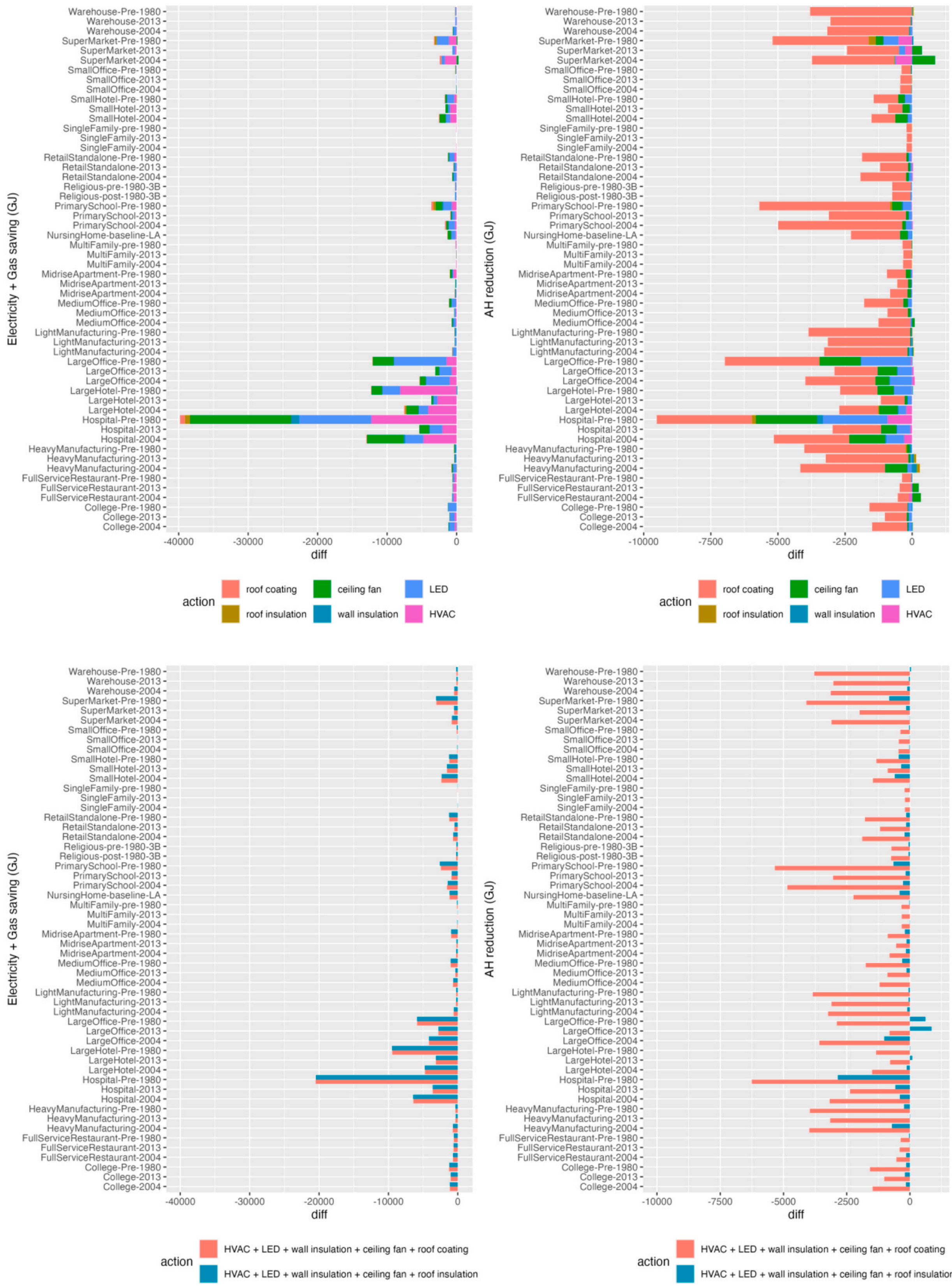

Fig. A2. Individual (top) vs package (bottom) retrofit effect on annual site energy (left) and summer AH (right).

A3. WRF model performance analysis

In this Appendix, we present Fig. A3, which illustrates the spatial distribution of model performance metrics for 2-meter-height air temperature.

The metrics shown include root mean square error (RMSE), Pearson correlation, and overall agreement between ground observations and model predictions. Ground observations were obtained from traditional weather stations in the ASOS/AWOS network. Fig. A3 summarizes how well the model reproduces observed near-surface air temperature over the study area.

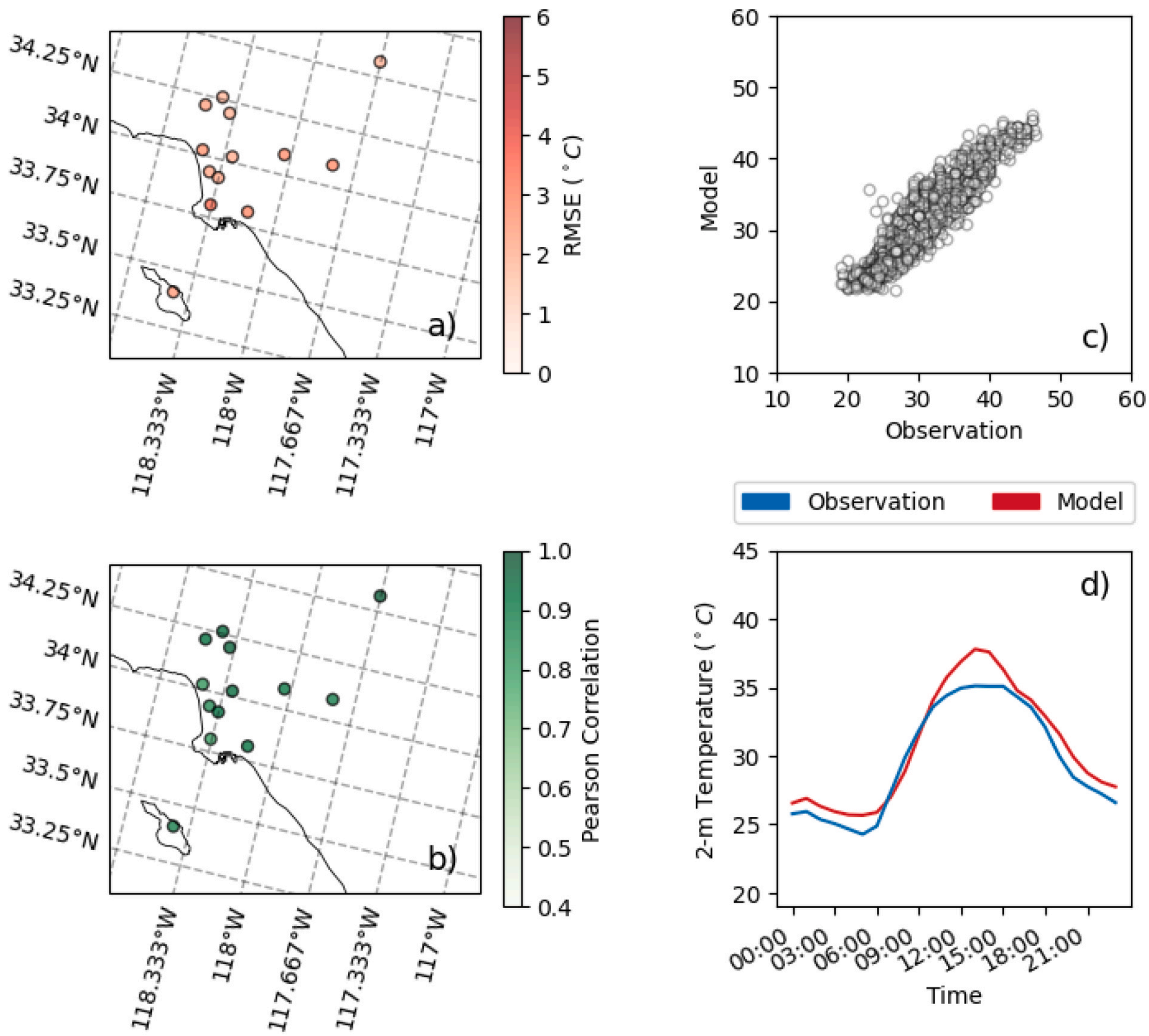

Fig. A3. Spatial distribution of (a) RMSE (°C), (b) Pearson correlation, and (c) overall agreement between ground observations and model prediction in capturing 2-m air temperature. (d) Spatially averaged diurnal temperature from ASOS/AWOS stations and the corresponding model predictions. Observation and model are shown in blue and red, respectively.

A4. Prototype Building Model Characteristics

Table A4
Prototype building characteristics.

Building Type	Number of Floors	HVAC Heating	HVAC Cooling	Primary System	Baseline HVAC Setpoints (Cooling / Heating)	Source
Single-Family	1	Gas furnace	Unitary DX		Cooling 25.6C / Heating 20.0C	CBES, generated based on California Title 24 building energy efficiency standards.
Multi-Family	2	Gas furnace	Unitary DX		Cooling 25.6C / Heating 20.0C	
College	4	Boiler	Chiller, cooling tower	VAV	Cooling 23.9C / Heating 21.1C	OpenStudio Standard Gem, generated based on ASHRAE 90.1 building energy efficiency standards.
Full-service Restaurant	1	Gas furnace	Unitary DX	CAV	Cooling 24.0C / Heating 21.0C	
Hospital	5	Boiler	Chiller, cooling tower	VAV w/ reheat	Cooling 24.0C / Heating 21.0C	
Large Hotel	6	Boiler	Air cooled chiller	Fan-coil units	Cooling 24.0C / Heating 21.0C	

(continued on next page)

Table A4 (*continued*)

Building Type	Number of Floors	HVAC Heating	HVAC Cooling	Primary System	Baseline HVAC Setpoints (Cooling / Heating)	Source
Large Office	12	Boiler	Chiller, cooling tower	VAV w/ reheat	Cooling 24.0C / Heating 21.0C	
Medium Office	3	Gas furnace	Unitary DX	VAV w/ elect. reheat	Cooling 24.0C / Heating 21.0C	
Midrise Apartment	2	Gas	Split DX	CAV	Cooling 24.4C / Heating 21.7C	
Primary School	3	Boiler / Gas furnace	Unitary DX	VAV w/ reheat	Cooling 24.0C / Heating 21.0C	
Standalone Retail	1	Gas furnace	Unitary DX	CAV	Cooling 23.9C / Heating 21.1C	
Small Hotel	4	Electricity	DX	PTAC	Cooling 23.9C / Heating 21.1C	
Small Office	1	Heat Pump	Unitary DX	CAV	Cooling 23.9C / Heating 21.1C	
Supermarket	1	Gas furnace	Unitary DX	RTU	Cooling 24.0C / Heating 15.6C	
Warehouse	1	Gas furnace	Unitary DX	Unit heater	Cooling 23.9C / Heating 21.0C	
Religious	2	PTAC	PTAC		Cooling 23.9C / Heating 20.9C	Prototype models were developed based on CBECS data Ye et al. [39].
Nursing Home	2	Boiler	Chiller, cooling towerSun et al. [40]	VAV	Cooling N/A C / Heating N/A C	Adapted from
Light Manufacturing	1	Gas furnace	Unitary DX	Unit heater	Cooling 23.9C / Heating 21.0C	Adapted from the warehouse models generated by the OpenStudio Standard Gem.
Heavy Manufacturing	1	Gas furnace	Unitary DX	Unit heater	Cooling 23.9C / Heating 21.0C	

A5. Heating and cooling system COP before and after HVAC upgrades

Table A5
Heating and Cooling system COP before and after upgrades.

Building Type	Baseline		HVAC replacement	
	Heating COP	Cooling COP	Heating COP	Cooling COP
College	0.8	5.1	1.8	5.1
Full-Service Restaurant	0.9	3.4	2.6	3.4
Heavy Manufacturing	0.9	3.5	0.9	3.5
Hospital	0.8	5.8	1.6	5.8
Large Hotel	0.8	2.8	1.8	2.8
Large Office	1.6	5.0	2.1	5.0
Light Manufacturing	0.9	3.5	0.9	3.5
Medium Office	0.9	3.3	1.7	3.3
Midrise Apartment	0.8	3.6	2.0	3.5
Multi-Family	0.8	2.6	2.8	2.6
Nursing Home	0.9	4.1	3.0	4.1
Primary School	0.9	3.4	2.9	3.4
Religious	0.8	3.1	2.8	3.1
Retail Standalone	0.9	3.4	3.0	3.4
Single-Family	0.8	2.6	2.8	2.6
Small Hotel	0.9	3.3	1.8	3.3
Small Office	1.6	3.6	2.2	3.6
Super Market	0.9	3.4	3.1	3.4
Warehouse	0.9	3.5	2.7	3.4

Data availability

Data will be made available on request.

References

[1] EIA, How much energy is consumed in U.S. buildings?. https://www.eia.gov/tools/faqs/faq.php?id=86&t=1.
[2] A. Block, K. Keuler, E. Schaller, Impacts of anthropogenic heat on regional climate patterns, Geophys. Res. Lett. 31 (12) (2004), https://doi.org/10.1029/2004GL019852.
[3] A.K.L. Quah, M. Roth, Diurnal and weekly variation of anthropogenic heat emissions in a tropical city, Singapore, Atmos. Environ. 46 (2012) 92–103, https://doi.org/10.1016/j.atmosenv.2011.10.015.
[4] D.J. Sailor, A review of methods for estimating anthropogenic heat and moisture emissions in the urban environment, Int. J. Climatol. 31 (2011) 189–199, https://doi.org/10.1002/joc.2106.
[5] P. Vahmani, X. Luo, A. Jones, T. Hong, Anthropogenic heating of the urban environment: an investigation of feedback dynamics between urban micro-climate and decomposed anthropogenic heating from buildings, Build. Environ. 213 (2022) 108841, https://doi.org/10.1016/j.buildenv.2022.108841.
[6] D.J. Sailor, M. Georgescu, J.M. Milne, M.A. Hart, Development of a national anthropogenic heating database with an extrapolation for international cities, Atmos. Environ. 118 (2015) 7–18, https://doi.org/10.1016/j.atmosenv.2015.07.016.
[7] R. Sun, Y. Wang, L. Chen, A distributed model for quantifying temporal-spatial patterns of anthropogenic heat based on energy consumption, J. Clean. Prod. 170 (2018) 601–609, https://doi.org/10.1016/j.jclepro.2017.09.153.

[8] T. Ichinose, K. Shimodozono, K. Hanaki, Impact of anthropogenic heat on urban climate in Tokyo, Atmos. Environ. 33 (24) (1999) 3897–3909, https://doi.org/10.1016/S1352-2310(99)00132-6.

[9] H. Taha, Urban climates and heat islands: albedo, evapotranspiration, and anthropogenic heat, Energy Build. 25 (1997) 99–103, https://doi.org/10.1016/S0378-7788(96)00999-1.

[10] G. Pigeon, D. Legain, P. Durand, V. Masson, Anthropogenic heat release in an old European agglomeration (Toulouse, France), Int. J. Climatol. 27 (2007) 1969–1981, https://doi.org/10.1002/joc.1530.

[11] C. Smith, S. Lindley, G. Levermore, Estimating spatial and temporal patterns of urban anthropogenic heat fluxes for UK cities: the case of Manchester, Theor. Appl. Climatol. 98 (2009) 19–35, https://doi.org/10.1007/s00704-008-0086-5.

[12] Y. Dong, A.C.G. Varquez, M. Kanda, Global anthropogenic heat flux database with high spatial resolution, Atmos. Environ. 150 (2017) 276–294, https://doi.org/10.1016/j.atmosenv.2016.11.040.

[13] D.J. Sailor, L. Lu, A top–down methodology for developing diurnal and seasonal anthropogenic heating profiles for urban areas, Atmos. Environ. 38 (2004) 2737–2748, https://doi.org/10.1016/j.atmosenv.2004.01.034.

[14] T. Hong, M. Ferrando, X. Luo, F. Causone, Modeling and analysis of heat emissions from buildings to ambient air, Appl. Energy 277 (2020) 115566, https://doi.org/10.1016/j.apenergy.2020.115566.

[15] X. Luo, P. Vahmani, T. Hong, A. Jones, City-scale building anthropogenic heating during heat waves, Atmos. 11 (11) (2020) 11, https://doi.org/10.3390/atmos11111206.

[16] Y. Xu, P. Vahmani, A. Jones, T. Hong, Anthropogenic heat from buildings in Los Angeles County: a simulation framework and assessment, Sustain. Cities Soc. 107 (2024) 105468, https://doi.org/10.1016/j.scs.2024.105468.

[17] S. Bienert, H. Kuhlwein, Y. Schmidt, B. Gloria, B. Agbayir, Embodied carbon of retrofits. Ensuring the Ecological Payback of, Energetic Retrofits (2023).

[18] W.J. Fisk, B.C. Singer, W.R. Chan, Association of residential energy efficiency retrofits with indoor environmental quality, comfort, and health: a review of empirical data, Build. Environ. 180 (2020) 107067.

[19] Z. Ma, P. Cooper, D. Daly, L. Ledo, Existing building retrofits: methodology and state-of-the-art, Energy Build. 55 (2012) 889–902, https://doi.org/10.1016/j.enbuild.2012.08.018.

[20] M. Ferrando, F. Causone, T. Hong, Y. Chen, Urban building energy modeling (UBEM) tools: a state-of-the-art review of bottom-up physics-based approaches, Sustain. Cities Soc. 62 (2020) 102408, https://doi.org/10.1016/j.scs.2020.102408.

[21] R.E. López-Guerrero, A.S. Cruz, T. Hong, M. Carpio, Optimizing urban housing design: improving thermo-energy performance and mitigating heat emissions from buildings–a Latin American case study, Urban Clim. 57 (2024) 102119.

[22] B. Maronga, M. Winkler, D. Li, Can areawide building retrofitting affect the urban microclimate? An LES study for Berlin, Germany, J. Appl. Meteorol. Climatol. (2022), https://doi.org/10.1175/JAMC-D-21-0216.1.

[23] W.C. Skamarock, J.B. Klemp, J. Dudhia, D.O. Gill, Z. Liu, J. Berner, W. Wang, J.G. Powers, M.G. Duda, D.M. Barker, A description of the advanced research WRF model version 4, National Center for Atmospheric Research, Boulder, CO, USA, (2019), p. 145.

[24] A. Martilli, Numerical study of urban impact on boundary layer structure: sensitivity to wind speed, urban morphology, and rural soil moisture, J. Appl. Meteorol. Climatol. 41 (2002) 1247–1266, https://doi.org/10.1175/1520-0450(2002)041<1247:NSOUIO>2.0.CO;2.

[25] T. Hong, M.A. Piette, Y. Chen, S.H. Lee, S.C. Taylor-Lange, R. Zhang, K. Sun, P. Price, Commercial building energy saver: an energy retrofit analysis toolkit, Appl. Energy 159 (2015) 298–309, https://doi.org/10.1016/j.apenergy.2015.09.002.

[26] LA County CIO, Assessor Parcels Data 2006 thru 2021, Open Data Portal County of Los Angeles (2022). https://data.lacounty.gov/search?categories=open%20data.

[27] Los Angeles Region Imagery Acquisition Consortium, Pictometry International Corp , LARIAC (2021). https://lariac-lacounty.hub.arcgis.com/.

[28] Y. Xu, P. Vahmani, A. Jones, T. Hong, A multi-scale time-series dataset of anthropogenic heat from buildings in Los Angeles County [Dataset], MultiSector Dynamics - Living, Intuitive, Value-adding, Environment (2022), https://doi.org/10.57931/1892041.

[29] A. Martilli, Numerical study of urban impact on boundary layer structure: sensitivity to wind speed, urban morphology, and rural soil moisture, J. Appl. Meteorol. Climatol. 41 (2002) 1247–1266, https://doi.org/10.1175/1520-0450(2002)041<1247:NSOUIO>2.0.CO;2.

[30] M.J. Iacono, J.S. Delamere, E.J. Mlawer, M.W. Shephard, S.A. Clough, W. D. Collins, Radiative forcing by long-lived greenhouse gases: calculations with the AER radiative transfer models, J. Geophys. Res. Atmos. 113 (2008).

[31] G. Thompson, P.R. Field, R.M. Rasmussen, W.D. Hall, Explicit forecasts of winter precipitation using an improved bulk microphysics scheme. Part II: implementation of a new snow parameterization, Mon. Weather Rev. 136 (2008) 5095–5115.

[32] A.S. Monin, A.M. Obukhov, Basic laws of turbulent mixing in the surface layer of the atmosphere, Contrib. Geophys. Inst. Acad. Sci. USSR 151 (1954) e187.

[33] F. Chen, J. Dudhia, Coupling an advanced land surface–hydrology model with the Penn State–NCAR MM5 modeling system. Part I: model implementation and sensitivity, Mon. Weather Rev. 129 (2001) 569–585.

[34] M.B. Ek, K.E. Mitchell, Y. Lin, E. Rogers, P. Grunmann, V. Koren, et al., Implementation of Noah land surface model advances in the National Centers for Environmental Prediction operational mesoscale Eta model, J. Geophys. Res. Atmos. 108 (2003).

[35] B. Bechtel, P.J. Alexander, J. Böhner, J. Ching, O. Conrad, J. Feddema, et al., Mapping local climate zones for a worldwide database of the form and function of cities, ISPRS Int. J. Geo-Inf. 4 (2015) 199–219.

[36] H. Hersbach, B. Bell, P. Berrisford, et al., The ERA5 global reanalysis, Q. J. R. Meteorol. Soc. 146 (2020) 1999–2049, https://doi.org/10.1002/qj.3803.

[37] P. Vahmani, A.D. Jones, Water conservation benefits of urban heat mitigation, Nat. Commun. 8 (2017) 1072, https://doi.org/10.1038/s41467-017-01346-1.

[38] NLR, ComStock, **National Laboratory of the Rockies (2020)**. https://comstock.nlr.gov/.

[39] Y. Ye, K. Hinkelman, J. Zhang, W. Zuo, G. Wang, A methodology to create prototypical building energy models for existing buildings: a case study on U.S. religious worship buildings, Energ. Buildings 194 (2019) 351–365, https://doi.org/10.1016/j.enbuild.2019.04.037.

[40] K. Sun, M. Specian, T. Hong, Nexus of thermal resilience and energy efficiency in buildings: a case study of a nursing home, Build. Environ. 177 (2020) 106842, https://doi.org/10.1016/j.buildenv.2020.106842.